China Instrument and Control Society
Instrumentation
INSTRUMENTATION, Vol. 11, No. 3, September 2024 https://doi.org/10.15878/j.instr.202400241

Article

Threat Assessment Method Considering Target Instantaneous and Historical States

Zhen Zuo, Peng Wu*, Xiaoyong Sun, Bei Sun, Shaojing Su

College of Intelligence Science and Technology, National University of Defense Technology, Changsha, Hunan, China

* Corresponding author email: Corresponding author email: pengwu@nudt.edu.cn

Abstract: The sea surface escort formation faces various threats in reality. For example, suicide boats may carry explosives or other dangerous items, aiming to cause maximum damage by colliding or detonating escort targets. Since suicide boats have a certain degree of concealment, it is necessary to establish a threat assessment algorithm to timely identify and respond to such fast and concealed threats. This paper establishes a threat assessment model that considers the instantaneous and historical states of the target. The instantaneous state of the target takes into account six evaluation indicators, including target category, target distance, target heading, target speed, collision risk, and ship automatic identification system (AIS) recognition status; in terms of historical state information mining, a target typical intention recognition method based on graph neural network is proposed to achieve end-to-end target typical intention recognition. Furthermore, this paper introduces a multi-attribute decision analysis method to weight the evaluation indicators, improves the relative closeness calculation method between different evaluation schemes and positive and negative ideal schemes, and determines the target threat ranking based on relative closeness. Based on Unity3D, a set of unmanned boat confrontation simulation system is designed and developed, and typical intention recognition data sets and threat assessment scenario simulation data are generated through real-life confrontation. Comparative analysis shows that the threat assessment model in this paper can accurately and timely detect raid target threats and give scientific and reasonable target threat ranking results.

Keywords: sea surface target; threat assessment; instantaneous status; historical status

Citation: Zuo, Zhen, Peng Wu, Xiaoyong Sun, Bei Sun, and Shaojing Su. "Threat Assessment Method Considering Target Instantaneous and Historical States." Instrumentation 11, no. 3 (September 2024). https://doi.org/10.15878/j.instr.202400241.

1 Introduction

Target threat assessment means judging the threat of the target to our intentions and purposes, and quantifying and obtaining intuitive understanding. Since unidentified targets on the sea surface have a certain degree of concealment, it is necessary to establish a threat assessment model to timely identify and respond to such rapid and concealed threats. Reasonable target threat assessment can timely discover and respond to potential threats. By identifying typical intentions and ranking target threats on the sea surface, it can more accurately determine which targets or areas need more attention and resources, provide important decision-making basis, and help formulate effective defense strategies or countermeasures. However, target threat assessment is a complex process with a large number of uncertain factors. How to quickly and comprehensively establish a threat assessment index system and determine the index weight coefficient is the key to scientific target threat assessment. Different evaluation index systems and different index weight coefficients may result in completely different final evaluation results, which will directly affect the rationality of target threat judgment.

Although the existing target threat assessment methods have achieved certain results and have been

successfully applied to target threat assessment, there are still many shortcomings, which are specifically reflected in the fact that the assessment process only considers the current instantaneous state information and ignores the information contained in the target's historical motion state[1,2]. Wang et al proposed threat assessment method considering instant speed, weapon, direction and type of targets[1]. Shu et al toke the type, weapon, speed, direction and distance of targets into consideration in the proposed threat assessment, which were also instant factors without historical states[2]. In the evaluation process, many methods only perform threat assessment based on the information of the target at the current moment, which makes the threat assessment fragmented and discrete, ignores the data information of multiple historical moments, and cannot reflect the dynamic changes of the target threat level in the complex and changeable battlefield situation. For example, as shown in Fig.1, consider the trajectory diagram of the unmanned boat escort formation and the unknown target under different time series. In the scene of Fig.1 (a), when the traditional method performs threat assessment on target 1 at time T_1, because its direction of travel is far away from the unmanned boat escort formation, the traditional method determines that the target is of low threat. Considering the trajectory diagram of target 1 from time T_0 to time T_1, it can be found that the target has an obvious typical circling tracking reconnaissance route. When conducting threat assessment, its threat value should be increased to a certain extent. In the scene of Fig.1 (b), both targets 2 and 3 are speedboats. Compared with the unmanned boat escort formation, their position and movement state at time T_1 are consistent with the speed, and the movement direction is a mirror image of the unmanned boat escort formation. When the traditional method performs threat assessment on the two targets at time T_1, it only considers the instantaneous state and gives the same threat level to the two targets. However, considering the movement trajectories of target 2 and target 3, the movement of target 2 has the phenomenon of repeated approach and distance, with higher uncertainty, while the movement of target 3 is relatively stable. Therefore, when conducting threat assessment on the two targets, the threat level of target 2 should be higher than that of target 3, and target 2 should receive more attention. When conducting threat assessment on targets, traditional methods do not model the deep intention information in the historical motion state of the target, and only rely on the current motion state of the target for threat assessment, and the target information mining is not sufficient.

In view of the shortcomings of the current target threat assessment methods analyzed above, this paper establishes a threat assessment model that considers the instantaneous and historical states of the target. It not only considers the instantaneous state factors of the target, but also establishes a target typical intention recognition model based on the historical state of the target. Taking the target intention recognition results into account, a threat affiliation function model is established for the evaluation index system, and the evaluation index is weighted based on multi-attribute decision analysis. Then, the relative closeness between the evaluation schemes of different targets and the positive and negative ideal schemes is calculated, and the target threat ranking is determined based on the relative closeness.

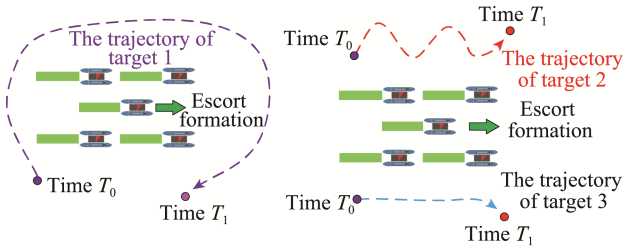

(a) Single target scene (b) Two targets scene

Fig.1 Trajectory diagram of the unmanned boat escort formation and unknown targets under historical conditions

Fig.2 is the overall framework of target threat assessment proposed in this paper. This paper establishes a threat assessment model that considers the instantaneous state and historical state of the target. The instantaneous state of the target considers six evaluation indicators such as target category, target distance, target heading, target speed, collision risk, and AIS response. In addition, this paper establishes a target typical intention recognition model based on the historical state, proposes a typical intention recognition method based on graph neural network, captures the dynamic correlation between the target and the escort formation, realizes end-to-end target typical intention recognition, and takes target intention as an evaluation indicator. Then, threat affiliation functions were established for the seven evaluation indicators, and the indicator values were normalized to [0,1]. The larger the value, the higher the threat level. Furthermore, the evaluation indicators were weighted based on multi-attribute decision analysis, and the relative closeness between the evaluation schemes of different targets and the positive and negative ideal schemes was calculated, and the target threat ranking was determined based on the relative closeness.

2 Related Works

In reality, the sea surface escort formation faces various threats. For example, suicide boats may carry explosives or other dangerous items, aiming to cause maximum damage by colliding or detonating the escort target. Since suicide boats have a certain degree of concealment, it is necessary to establish a set of threat assessment algorithms to timely identify and respond to such fast and hidden threats. In order to more comprehensively perceive the information of sea surface targets, the unmanned boat sea surface escort mission needs to efficiently and accurately grasp and predict the status of enemy sea targets and conduct threat assessment on sea targets. Reasonable target threat assessment can

timely discover and respond to potential threats. By conducting threat assessment and target threat ranking on sea surface targets, it can more accurately determine which targets or areas require more attention and resources, provide important decision-making basis, and help formulate effective defense strategies or countermeasures [1,3]. Target threat assessment refers to judging the threat of the target to our intentions and purposes, and quantifying and obtaining intuitive understanding. However, the target threat assessment process is relatively complex, and the assessment results are easily affected by many different factors. How to quickly and comprehensively establish a threat assessment index system and determine the index weight coefficient is the key to scientific target threat assessment [4]. As shown in Fig.3, threat assessment can usually be divided into three steps: establishing a threat assessment indicator system, calculating indicator weight coefficients, and ranking target threats [5]. This article will summarize the domestic and international research status of the above three steps respectively.

2.1 Threat Assessment Indicator

The first step in maritime target threat assessment is to establish a threat assessment index system. The current index system mainly focuses on instantaneous state factors. Chen Xingle et al. selected four types of target feature information, namely target distance, target heading, target speed and target collision risk, and established a threat assessment index system. However, the system only targets the single case of target collision and does not consider more complex situations[6]. Gong Hua proposed comprehensive method considering two terms of the target threat including threat degree and threat range[7]. Shu Jiansheng et al. took into account

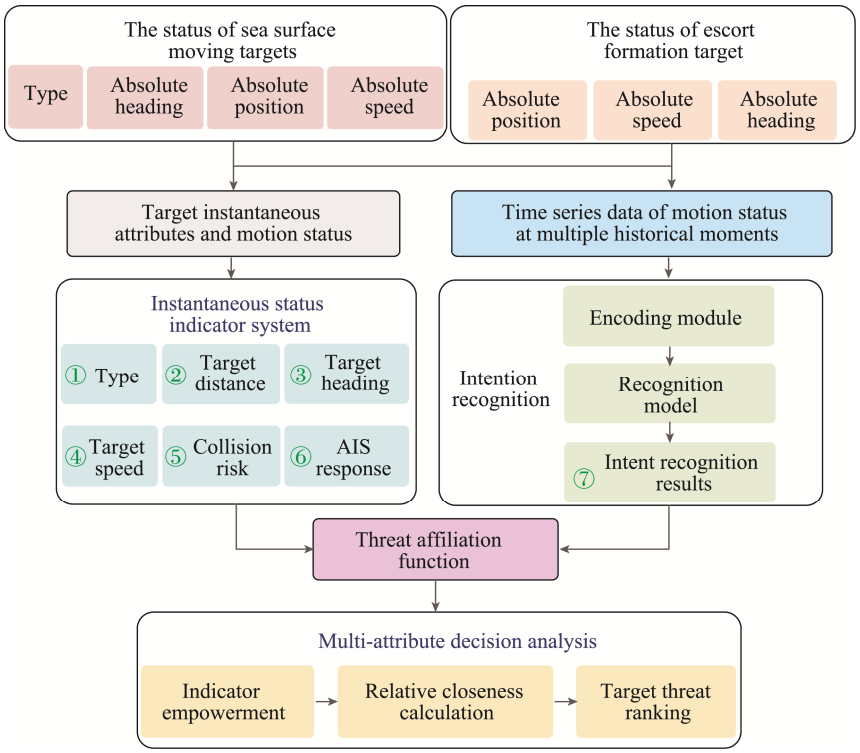

Fig.2 The overall threat assessment framework in this paper

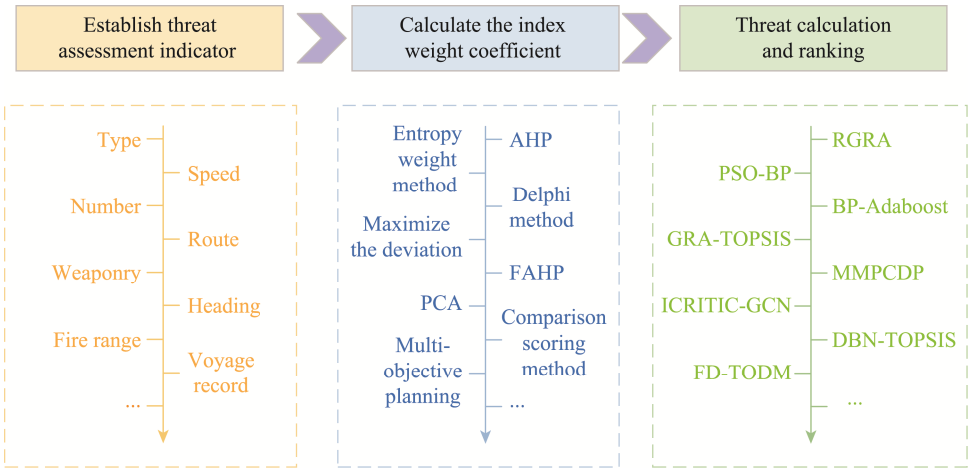

Fig.3 Current status of sea surface target threat assessment methods

the weapon configuration of the ship and proposed a five-index evaluation system including target type, weapon configuration, target distance, target entry angle and target speed, further optimizing the target feature information evaluation model[2]. The threat assessment index system established by Zhao et al. takes into account the combat capability of the incoming target, where the target combat capability includes target type and maneuverability[8]. Based on quantitative and qualitative analysis methods, Shi et al. selected three static indicators, namely target type, lethality and jamming capability, for qualitative analysis, and selected five dynamic indicators, namely target number, speed, altitude, range and heading angle, for quantitative analysis[9]. Chen Kaiyuan et al. fully considered the maritime combat situation and listed 14 indicators, namely target type, target distance, target origin and destination, target number, target route, target speed, navigation record, closest distance, coordinated action, radiation source signal, weapon range, friendly support, communication status and cargo, aiming to judge the threat level of the target as accurately as possible. However, due to the complexity of the indicator system, it is difficult to assign scientific and reasonable weights to the indicators[10].

2.2 Calculation of indicator weight coefficients

After establishing the threat assessment index system, it is necessary to calculate the weight coefficient of each index to characterize the relative proportion of the index, so as to comprehensively evaluate the target threat level by combining the results of multiple evaluation indicators. When the threat assessment model and the evaluation index value are the same, but the weights of one or more evaluation indicators are different, the target threat assessment results may be completely different. At present, the weight coefficient calculation methods mainly include subjective weighting methods that rely on decision maker preferences and expert experience, objective weighting methods that rely on mathematical models and target attribute data, and combined weighting methods that integrate decision maker preferences and objective data. Among them, the analytic hierarchy process (AHP) and the year-on-year scoring method are typical representatives of subjective weighting methods, while the entropy weight method and the principal component analysis method are typical representatives of objective weighting methods. Xiao Jun used the analytic hierarchy process in the subjective weighting method to solve the weights. By making full use of the information of different level intervals and optimizing the interval weight calculation strategy, he obtained a more scientific and reasonable target threat assessment result[11]. Zhang Huan proposed examples of analysis of target threat assessment based on SVM[12]. Wang Zeyan et al. proposed an objective weighting method based on maximum deviation and entropy from a purely objective perspective, and introduced entropy to describe the uncertainty caused by the randomness of weight coefficients. Wang Changjin et al. used a combined weighting method based on subjective analytic hierarchy process and objective information entropy method to determine the weight coefficients of each indicator in the proposed threat assessment model, so that the final threat assessment results contain both subjective information and objective characteristics[13]. Lin et al. proposed an attribute weight coefficient optimization model to reduce the total deviation between objective preference (attribute value) and subjective preference value, making the decision more reasonable [14]. Hong et al.[15] proposed a target threat assessment model based on combined weights to address the problem of uneven distribution of indicator weights in combat threat assessment. The model uses analytic hierarchy process and key method to determine the subjective weight and objective weight of indicators, and uses multiplication synthesis method to calculate the combined weight. In order to solve the problems of difficulty in data analysis, high subjectivity, and rigid priority logic in multi-target threat assessment, Yu et al. proposed the PROMETHEE algorithm, which is based on the fusion weights of entropy and analytical network process (ANP) calculations. This algorithm fully considers the influence of subjective and objective factors on problem analysis and improves the rationality of threat assessment[16].

2.3 Calculation of target (absolute or relative) threat

After obtaining the target threat index set and the weight coefficients of each index, the threat assessment method can be used to calculate the absolute or relative threat level of the target and give the target threat ranking results to provide a reference for the next step of threat target disposal, strike decision-making, etc. Absolute threat level refers to the threat measurement of the target itself. This assessment does not consider the existence of other targets and is a direct evaluation of the threat of a single target; relative threat level is when considering the existence of multiple targets. This assessment involves comparing and ranking the threats of each target to determine which targets should be given priority in the current situation. Existing threat assessment algorithms mainly include multi-attribute decision-making algorithms, Bayesian network algorithms, fuzzy theory algorithms, genetic algorithms, neural network algorithms, and grayscale correlation algorithms. José et al. proposed a threat assessment system based on information fusion from different sources. The system implements target threat level assessment based on Bayesian networks[17].

Ehsan et al. proposed a new threat assessment method based on fuzzy evidence theory. By combining Dempster Shafer and fuzzy set theory, the uncertainty of sensor and system input data is considered to achieve dynamic target threat assessment. This method is real-time and can give reasonable, effective and reliable target threat assessment results[18]. Niu Shaoyuan performed a reasonable threat assessment based on the

information uploaded by its own sensors, and toke corresponding decisions based on the threat assessment[19]. Wang Baihe et al. proposed an improved grey correlation algorithm to evaluate target threats. This method improved the system evaluation efficiency, but did not consider the uncertainty information in the sample data and did not unify the subjective and objective weighting[20]. Chen Hua et al. introduced the Particle Swarm Optimization-Back Propagation (PSO-BP) algorithm into target threat assessment, solving the problem of BP network falling into local minima, and did not consider the complex relationship between threat factors[21]. Zhang Feng et al. used BP neural network as a weak predictor and performed ensemble learning through Adaboost to establish a BP-Adaboost strong predictor target threat estimation model, solving the problem of difficult network structure selection and poor generalization ability when predicting and estimating with a single neural network[22]. Xi Zhifei et al. proposed the Grey Relational Analysis-TOPSIS (GRA- TOPSIS) method. By introducing GRA to reflect the internal change rules of each scheme, it makes up for the shortcomings of TOPSIS. At the same time, it uses grey correlation and Euclidean distance to obtain relative closeness, and determines the target threat ranking based on relative closeness[23]. Li Ye proposed a dynamic programming Bayesian Network (BN) structure learning algorithm for improving Max-Min Parents and Children (MMPC). This algorithm can retain the causal relationship between each indicator and mine more implicit information[24]. Liu Fang et al. proposed a fusion threat assessment method DBN-TOPSIS based on dynamic Bayesian and approximate ideal solution. This method solves the problems of strong subjectivity, weak stability and discontinuous assessment process of threat assessment methods, and comprehensively considers the target motion characteristics and target attributes[25]. Based on mixed situation information and taking into account the limited rationality of decision makers and the differences in individual behaviors, Zhang Kun et al. proposed a fuzzy dynamic interactive multi-criteria decision-making algorithm FD-TODIM. The algorithm mines state information and generates threat assessment results with practical significance based on the individual differences of different decision makers[26].

2.4 Intention Recognition

There are many pattern recognition methods for target intention recognition, such as Bayesian networks[27,28], evidence reasoning[29], discriminant analysis[30], expert systems[31,32], decision trees (DTs)[33], D-S evidence theory[34], time windowing[35], and support vector machines (SVMs)[36]. Jin et al. used Bayesian network parameters based on the knowledge of military experts, which used the node characteristics to represent the transfer relationship. In this approach, the conditional probability represents the strength of the relationship, and the network parameters are updated using the influence of new events on backpropagation until the probability of an intention exceeds the threshold[37]. As artificial intelligence[38,39], data fusion[40,41], and deep learning[42-45] have developed, many intelligent intention recognition methods have been proposed. Zhou et al. combined the advantages of long short-term memory (LSTM) networks and DTs, to create an effective and feasible method for the state prediction and intention recognition of targets under uncertain and incomplete information[46]. Wei et al. proposed an intention recognition method based on a radial basis function neural network. Appropriate features are selected as the inputs of the neural network, which has adaptive and self-learning abilities for inferring the intention of the enemy[47].

3 Methods

3.1 Target state modeling and threat affiliation function

3.1.1 Target instantaneous state modeling and threat affiliation function

The selection of instantaneous state indicators for sea surface target threat assessment should fully consider the complexity and variability of the sea surface environment, and strive to consider various possible situations from multiple perspectives. Since threat assessment must be a real-time processing process, and prior knowledge cannot reflect the dynamic changes of the battlefield situation, they cannot be used as a direct source of information for sea surface target threat assessment. Based on the above analysis, considering the complex maritime situation, this paper selects 6 instantaneous state indicators, including target category, target distance, target heading, target speed, collision risk, and AIS response. Among them, target distance, target heading, and target speed are all relative values. Based on the theory of fuzzy mathematics, this paper constructs a threat affiliation function to normalize the data of different evaluation indicators to [0,1]. The larger the value, the higher the threat level. The affiliation function reflects the threat level under different indicators.

(1) Target categories

The sea surface environment is complex and changeable. Different types of sea surface targets have different functional tasks and the degree of threat to the escort targets also varies. The following is an analysis of the types of targets and their characteristics that the unmanned boat escort formation may encounter during the execution of the mission. It is worth noting that different types and threat affiliations can be set in different scenarios and flexibly adjusted according to actual conditions. The target categories comprehensively consider the types of warships and civilian ships, a total of 9 categories, from high to low in terms of threat level: warships, supply ships, speedboats, tugboats, cargo ships, sand carriers, fishing boats, cruise ships, sailboats, etc. It is worth noting that the target category evaluation index needs to be comprehensively judged with the sixth

indicator of the AIS response situation in this article, and each indicator is not independent.

Table 1 Different types of sea surface target ships and their threat affiliation

Ship Type	Speed range (m/s)	Threat Affiliation
warship	8-16	0.9
Supply ship	8-16	0.8
Speedboat	5-30	0.7
Tugboat	5-15	0.6
Sand carrier	5-12	0.5
Cargo ship	6-12	0.4
Fishing boat	2-5	0.3
Cruise boat	2-5	0.2
Sailboat and others	1-5	0.1

(2) Target distance

Target distance is an essential factor to consider in threat assessment. The distance between the surface target and the escort target can reflect the threat level of the target to the escort target to a certain extent. Generally, the greater the target distance, the less likely it is that the target will be successfully attacked. The target distance is negatively correlated with the threat level. The greater the target distance, the lower the threat level, and the smaller the target distance, the higher the threat level.

This paper defines the threat affiliation function of the distance between the sea surface target and the escort target as:

$$f_d=\begin{cases}1, & d\leqslant d_{\text{warning}}\\ \dfrac{(\lambda e)^{\frac{d_{\text{safe}}-d+d_{\text{darning}}}{d_{\text{safe}}}\times\mu}-1}{(\lambda e)^{\mu}-1}-1, & d_{\text{warning}}<d\leqslant d_{\text{safe}}\\ 0, & d>d_{\text{safe}}\end{cases} \quad (1)$$

Where, d is the actual distance between the sea target and the escort target, d_{safe} is a pre-set parameter, indicating the safety distance. When the target distance d is greater than d_{safe}, the threat affiliation is 0; d_{warning} is a pre-set parameter, indicating the warning distance. When the target distance d is less than d_{warning}, the threat affiliation is 1; λ and μ are compensation coefficients. When the safety distance is 1000m, the warning distance is 400 m, the compensation coefficient λ is 3.5, and the compensation coefficient μ is 3, the threat affiliation function graph is shown in Fig.4.

(3) Target heading

The target heading considered in this paper is the relative heading of the sea surface target relative to the escort target. The calculation of the relative heading of the sea surface target is shown in Fig.5.

v_1 and v_2 are the absolute velocity vectors of the escort target and the sea surface target (relative to the world reference system), respectively. Taking the escort target as the reference system, the velocity vector of the sea surface target relative to the escort target is v_R, and the line connecting the sea surface target and the escort target is the straight line in the facing direction. For the convenience of discussion, the clockwise direction is positive, and the target heading angle is $\theta\in[-180°,180°]$. When θ is smaller, the threat affiliation is greater; conversely, when θ is larger, the threat affiliation is smaller.

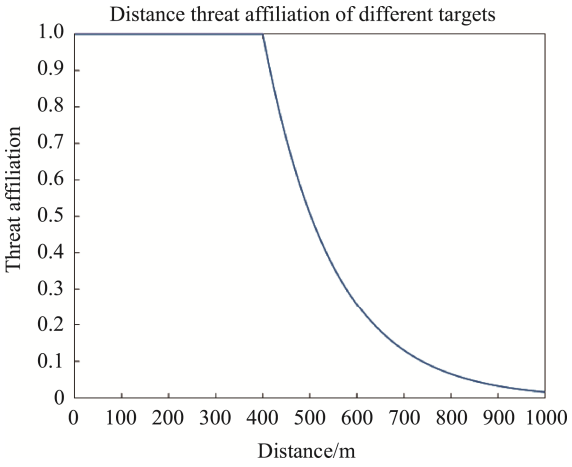

Fig.4 Distance threat affiliation function graph

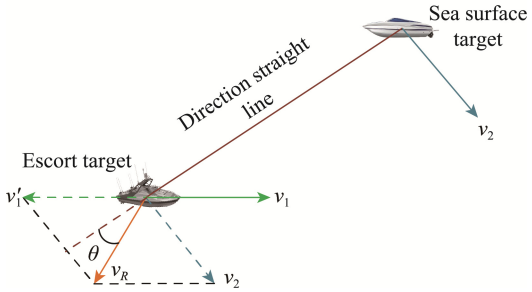

Fig.5 Schematic diagram of target heading calculation

The threat affiliation function of the target heading is a normal distribution:

$$\mu(\theta)=\mathrm{e}^{-k\theta^2} \quad (2)$$

Among them, $k=0.001$, the heading angle unit is degree. Fig.6 is a diagram of heading angle threat affiliation function.

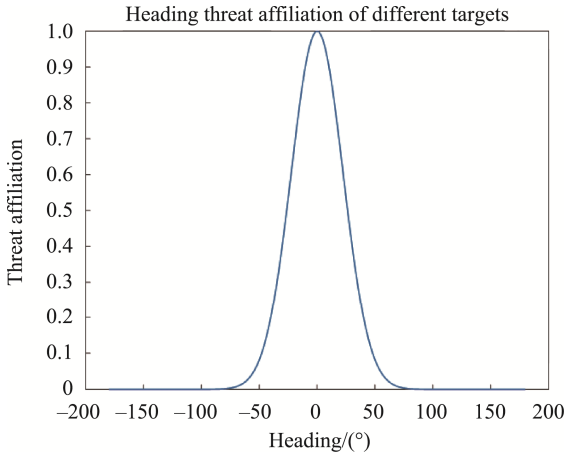

Fig.6 Heading angle threat affiliation function image

(4) Target speed

The target speed considered in this paper is the relative speed of the target relative to the escort target. The speed of the surface target relative to the escort target can, to a certain extent, reflect the threat posed by the target to the escort target. For example, targets such as suicide boats usually launch rapid raids, sometimes at speeds of more than 30 knots, attempting to carry out explosive attacks on the escort target when the escort formation fails to take countermeasures. Pirate speedboats also have similar action characteristics. Generally, the greater the target speed, the higher the probability of a successful raid. The target speed is positively correlated with the threat level. The greater the target speed, the higher the threat level, and the smaller the target speed, the lower the threat level. It is worth noting that the target speed is the speed component of the relative speed of the surface target and the escort target projected onto the straight line in the opposite direction. The relative relationship is shown in Fig.5. The target speed reflects the change in the straight-line distance between the surface target and the escort target. The threat affiliation function of the target speed is defined as:

$$f_v=\begin{cases}0, & g<0\\ g, & 0\leqslant g<1\\ 1, & g\geqslant 1\end{cases} \tag{3}$$

$$g=\left(\frac{\cos\theta\times v_R}{v_{\text{warning}}}\right)^{\xi} \tag{4}$$

In the formula, v_R represents the relative speed between the sea surface target and the escort target; v_{warning} is a pre-set parameter, which represents the warning speed. When the speed component of v_R on the straight line between the sea surface target and the escort target is greater than v_{warning}, the threat affiliation is 1; when $g<0$, $\cos\theta<0$, which represents $|\theta|$ between 90° and 180°, indicating that the sea surface target is moving away from the escort target at this time, and the threat affiliation is 0.

When the warning speed is 50m/s, is a coefficient greater than 1, and when ξ takes 3, the threat affiliation function diagram is shown in Fig.7.

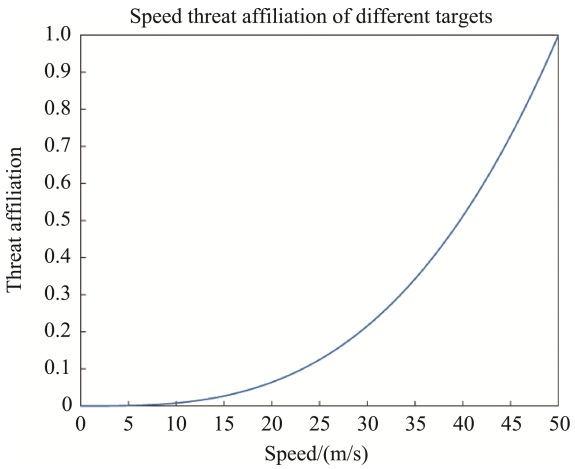

Fig.7 Speed threat affiliation function graph

(5) Collision risk

During sea navigation, some hostile targets will quickly approach or even collide with the escort formation. For example, suicide ships usually need to collide to threaten the escort target. The collision risk can be used to measure the threat of collision and provide early warning. The relative positions of the escort target and the sea target are shown in Fig.8.

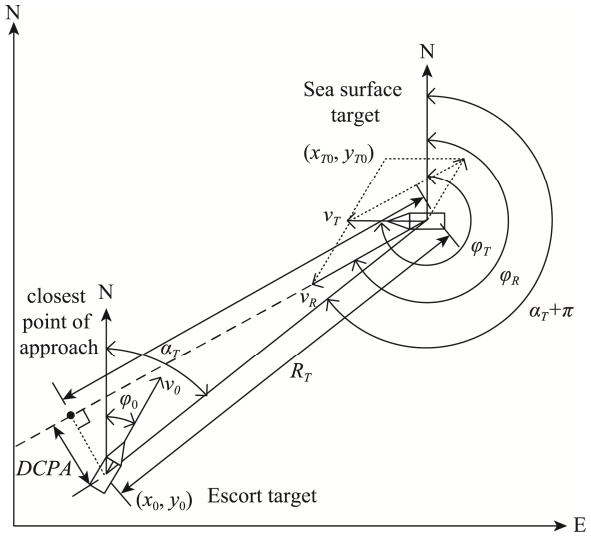

Fig.8 Relationship between the escort target and the sea surface target position

The black point in the figure is the position point where the sea target is closest to the escort target when passing by, that is, the closest encounter point.

The distance between the closest encounter point and the escort target is DCPA, which is calculated as follows:

$$\begin{cases}v_{x0}=v_0\cdot\sin\varphi_0\\ v_{y0}=v_0\cdot\cos\varphi_0\end{cases}\quad\begin{cases}v_{xT}=v_T\cdot\sin\varphi_T\\ v_{yT}=v_T\cdot\cos\varphi_T\end{cases} \tag{5}$$

$$\begin{cases}v_{xR}=v_{xT}-v_{x0}\\ v_{yR}=v_{yT}-v_{y0}\end{cases} \tag{6}$$

$$\varphi_R=\arctan\frac{v_{xR}}{v_{yR}}+\alpha \tag{7}$$

$$v_R=\sqrt{v_{xR}^2+v_{yR}^2} \tag{8}$$

$$R_T=\sqrt{\left(x_{T0}-x_0\right)^2+\left(y_{T0}-y_0\right)^2} \tag{9}$$

$$\alpha_T=\arctan\frac{x_{T0}-x_0}{y_{T0}-y_0}+\alpha \tag{10}$$

$$DCPA=R_T\cdot\sin\left(\varphi_R-\alpha_T-\pi\right) \tag{11}$$

Wherein, the angle is measured clockwise from the true north direction, and α is related to the numerator and denominator in arctan(). When the numerator $\geqslant 0$ and the denominator >0, α is 0°; when the numerator <0 and the denominator <0, α is 180°; when the numerator $\geqslant 0$ and the denominator <0, α is 180°; when the numerator <0 and the denominator >0, α is 360°. (x_0, y_0) are the X-axis and Y-axis coordinates of the escort target, v_0 is the actual

speed of the escort target, φ_0 is the actual heading of the escort target; (x_{T0}, y_{T0}) are the X-axis and Y-axis coordinates of the surface target, v_T is the actual speed of the surface target, φ_T is the actual heading of the surface target; φ_R and α_T are relative values, φ_R represents the relative heading of the surface target and the escort target, α_T represents the relative azimuth of the surface target and the escort target.

DCPA is used to quantify the size of the collision possibility, thereby constructing a collision risk model. The collision risk model defined in this paper is constructed using three variables: DCPA, d_1 and d_2, where d_1 represents the minimum safe encounter distance, and d_2 represents the zero boundary of the collision risk, usually $d_2 \approx 2d_1$[48]. Fig.9 is the graph of the collision risk membership function, and the collision risk u_{dT} is defined as:

$$u_{dT}=\begin{cases}1, & |DCPA|<d_1\\ \left(\dfrac{d_2-|DCPA|}{d_2-d_1}\right)^{3.03}, & d_1\leqslant|DCPA|\leqslant d_2\\ 0, & d_2<|DCPA|\end{cases} \quad (12)$$

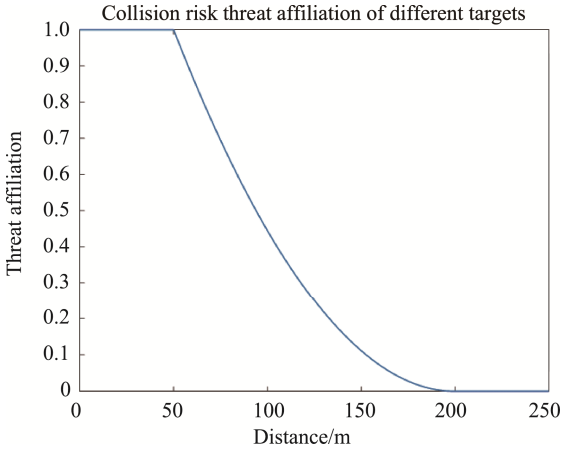

Fig.9. Collision risk threat affiliation function graph

(6) AIS response status

Most sea targets such as warships, cargo ships, cruise ships, tugboats, etc. are equipped with AIS response systems and can be responded and identified under normal circumstances. Unidentified ships such as suicide boats, pirate speedboats, illegal fishing boats, etc. are usually not responded and identified. In addition, the AIS systems of some foreign warships are turned off and cannot be responded and identified. Generally, the threat level of ship targets whose true legal identities can be identified through the AIS response system is low. When AIS responds and can be identified, the threat affiliation is defined as 0.2; when AIS does not respond and cannot be identified, the threat affiliation is defined as 0.8.

3.1.2 Modeling of target typical intention recognition based on historical status

Threat assessment based only on the current instantaneous state of the target cannot fully describe the target. Data information at multiple historical moments can reflect information such as the target's intention to a certain extent. For example, when an unknown surface target remains relatively still with the formation for a long time, or follows the escort formation to perform synchronous turning, acceleration and deceleration, etc., it may be that the ship is following before launching an attack, which requires special attention. This paper establishes a target typical intention recognition model based on graph neural network to capture the dynamic correlation characteristics between the target and the escort formation, and realize end-to-end target typical intention recognition. Based on the analysis of the changes in the motion state information of the surface target and the escort target at multiple moments in the time dimension, its behavioral intention is identified, and it is used as an evaluation indicator of the threat assessment model, combined with the instantaneous state indicator defined in Section 3.1.1 for target dynamic threat assessment.

(1) Analysis of typical target intentions

The definition of "intention": "the basic idea and intention to achieve a certain purpose". The meaning of intention recognition is to comprehensively analyze various target information sources to interpret and judge the purpose, idea and intention of the target. Referring to the definitions of several typical terms, according to different sea surface target characteristics and actual scenarios, this paper sets five typical target tactical intentions, such as assault, interception, harassment, tracking, and retreat, and others (i.e. no obvious intention), for a total of six typical target intentions. Among them, "others" means that the sea surface target has no obvious tactical intention and the threat level is low. For example, some sea surface targets pass through the sea area near the escort formation at a safe distance without obvious tactical behavior. The tactical intention of the target is non-numerical data and needs to be digitized. The corresponding relationship between the intention space, label and threat affiliation is shown in Fig.10.

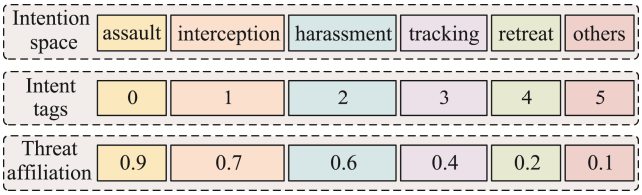

Fig.10 Correspondence between intent space, label and threat affiliation

Regarding assault intention, "Military Language" divides assault intention terminology into detailed categories such as frontal assault and flank assault. Assault is defined as "an attack on a combat deployment or action formation", among which close-range assault is contact-type, such as the collision attack of suicide boats. The typical frontal assault intention movement trajectory is shown in the trajectory of target 1 in Fig.11. The target generally goes straight to the escort target, with a fast speed or

accelerated maneuvering state, with the highest threat level and the greatest threat to the escort target. Its threat affiliation is defined as 0.9. Interception intention is generally defined as the target's interception and blockade against our side. The typical interception intention trajectory is shown in the trajectory of target 2 in Fig.11. The difference between interception intention and assault intention is that assault has the risk of direct collision, while interception is the tendency to coerce the other party to stop moving. The threat affiliation of interception intention is defined as 0.7. The harassment intention is generally defined as an action to disturb and restrain the opponent. In the sea scene, it is manifested as repeatedly approaching and moving away from the opponent in a certain pattern to achieve the purpose of repeatedly distracting the opponent's attention. The intention can be changed in time, and the intentions such as assault and retreat can be implemented in a short time. The threat affiliation of the harassment intention is defined as 0.6. The typical harassment intention trajectory is shown in Target 3 in Fig.11. The tracking intention is generally defined as an action to observe and continuously measure the target. In the sea scene, it is manifested as keeping a close distance with the opponent for a long time and performing similar maneuvers. Its threat affiliation is defined as 0.4, and the typical intention trajectory is shown in Target 4 in Fig.11. The retreat intention is generally defined as withdrawing from the conflict or possible conflict, withdrawing in a planned manner, and moving away from the opponent's target. The threat degree of this intention is relatively low, and the threat affiliation is defined as 0.2. The typical intention trajectory is shown in the trajectory of Target 5 in Fig.11. Regarding other intentions, it means that the sea surface targets have no obvious tactical intentions and the threat level is low. For example, some sea surface targets pass through the sea area near the escort formation within a certain range without obvious tactical behavior. The threat affiliation is defined as 0.1. The typical intention trajectory is shown in target 6 in Fig.11.

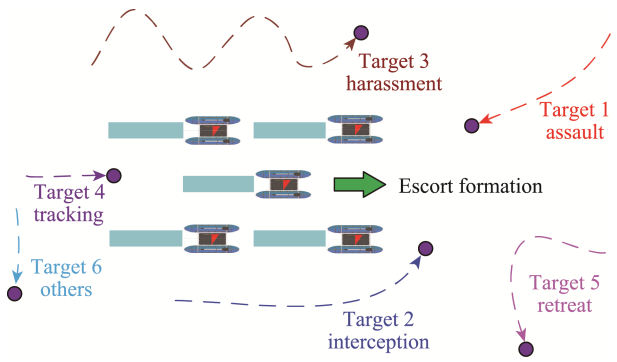

Fig.11 Schematic diagram of typical target intention

(2) Target Typical Intention Recognition Model Based on Graph Neural Network

In the actual sea environment, when the sea target has a specific intention towards the escort target, its motion state will change with the change of the escort target's motion state. Therefore, it is necessary to comprehensively consider the state sequence information at historical moments to determine the sea target's intention towards the escort target. This paper proposes a target typical intention recognition model combined with historical states, and the overall block diagram is shown in Fig.12.

The intention recognition method proposed in this paper considers the motion status of the escort formation target and the sea surface target at the current and historical moments at the same time. The sliding time window method (sliding window length is p+1) is used to send the motion status (including position, speed, and direction) of the escort formation target and the sea surface target at the current moment t and the past p historical moments into the encoder for encoding, and the motion coding features of the escort formation target and the sea surface target are obtained respectively. Then, the motion coding features of the escort formation target and the sea surface target are respectively sent to the difference feature extraction module and the dynamic association feature extraction module based on the graph neural network, and the features extracted by the two modules are concated; finally, the concated features are passed through the MLP layer and softmax to obtain the final intention recognition result. The loss function is CrossEntropyLoss.

The encoder module in this paper adopts the encoder part of Transformer. The structure of Transformer model is modular, and it is generally divided into two parts: encoder and decoder. The encoder mainly converts the input state sequence information into a higher-dimensional implicit feature vector. The encoder extracts the implicit correlation between the sea surface target and the escort formation target in their respective time series. The encoded features are used as the input of the subsequent feature extraction network. The complete encoder consists of multiple identical encoding modules, and each encoding module is composed of a multi-head self-attention layer module, a feedforward neural network module, and a residual and normalization module in a certain order. The core is the self-attention module. The original input of the encoding module is the motion state information of multiple targets over a period of time, so it needs to be quantized into a computable matrix. This process is the input embedding in the figure.

In order to adapt to the typical intention recognition of the time-varying number of sea surface targets, in the specific implementation of the algorithm, the maximum number of sea surface targets is preset to be N_T, the maximum total number of USVs and escort targets in the escort formation is N_U, the length of the sliding time window is L_T(L_T=p+1), and the motion state of all targets at each moment is a D_1·(D_1=1)-dimensional vector (X/Y coordinate position, velocity scalar and direction). When the number of sea surface targets or the number of escort formation targets in the actual scene is less than N_T or N_U, the mask layer is used to ignore the redundant input. The feature dimension input to the encoder is [B, N, L_T, D_1],

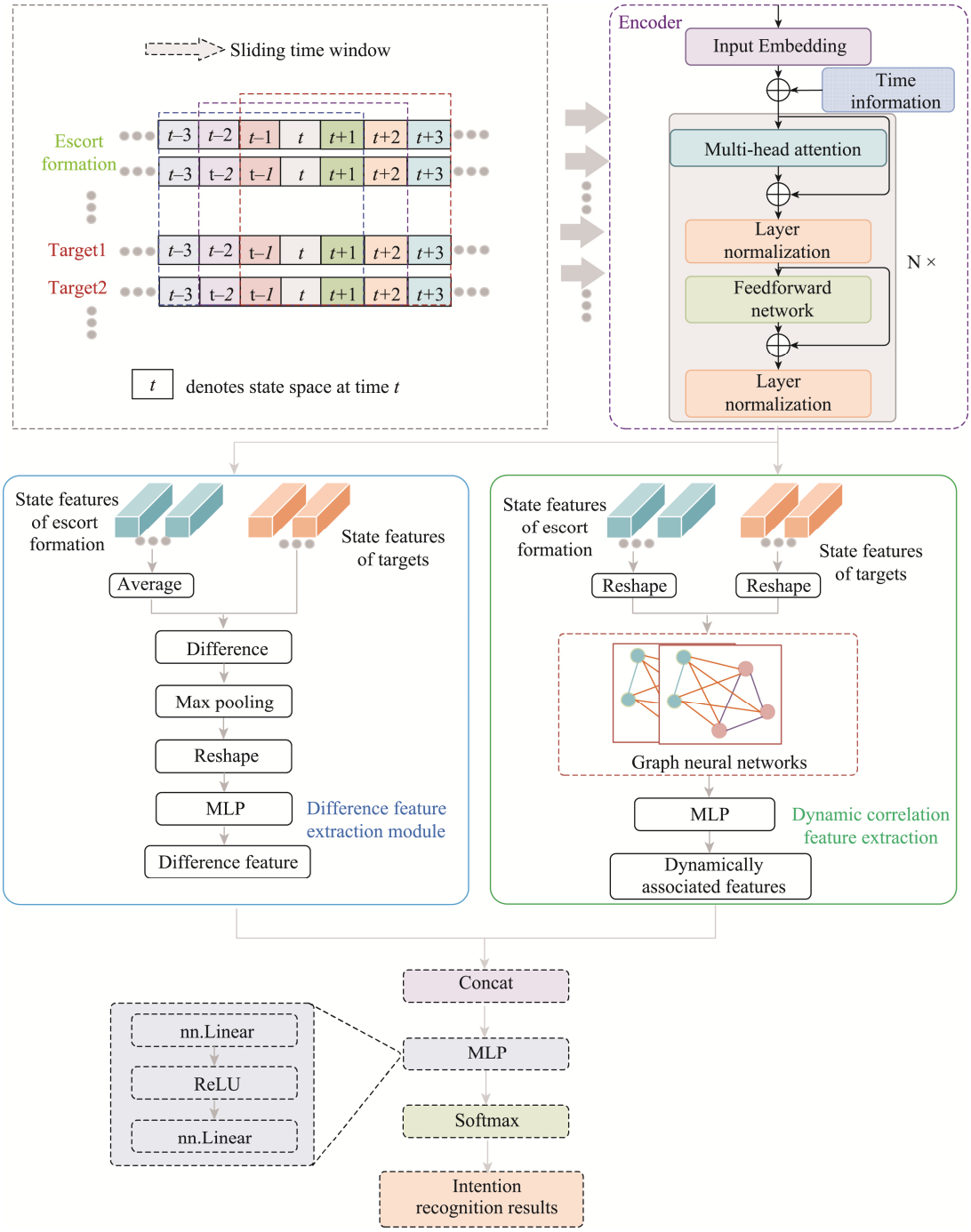

Fig.12 Overall block diagram of the target typical intention recognition model based on graph neural network

where $N=N_T+N_U$, B is the batch size. Since N_T and N_U are the maximum number of sea surface targets and escort formation targets preset, assuming that the number of sea surface targets and escort formation targets in an actual scene is N_T^r and N_U^r, the target intention label in this scene only corresponds to N_T^r sea surface targets. The feature dimension after the encoder is $[B, N, L_T, D_2]$, and the motion state sequence information is converted into a higher-dimensional implicit feature vector, and the encoder extracts the implicit association between sea surface targets and escort formation targets in their respective time series. The L_T state vector of each sea surface target and escort formation target at each moment is encoded into a feature vector of $[L_T, D_2]$ dimension , and the encoded features are used as the input of the difference feature extraction module and the dynamic association feature extraction module.

3.2 Threat Assessment Based on Multi-Attribute Decision Analysis

In Section 3.1, this paper established a target threat assessment index system, including instantaneous state indicators (target category, target distance, target heading, target speed, collision risk, AIS response status) and target typical intentions based on historical status, totaling 7

indicators. Based on the above indicator evaluation system, this section establishes a multi-attribute decision analysis model, calculates the weight of the dynamic evaluation index at each moment according to the entropy weight method, and then uses the improved approximate ideal solution method to calculate the relative closeness of different targets. Among them, this paper proposes a method of calculating relative closeness based on Euclidean distance and gray correlation weighted calculation, which can more objectively distinguish the threat level of different targets. Relative closeness reflects the relative threat level of different targets, and then the target threat ranking and dynamic analysis are performed based on the relative closeness.

First, construct an evaluation matrix. Assume that there are m evaluation schemes, the set of evaluation schemes is $G=\{G_1, G_2, \ldots, G_m\}$, the set of indicators composed of evaluation indicators is $T=\{T_1, T_2, \ldots, T_n\}$, and the attribute value of the evaluation object G_i corresponding to the indicator T_j at time t is x_{ij}^t, then the evaluation matrix of the evaluation object with respect to the evaluation indicator is $X_t=\left(x_{ij}^t\right)_{m\times n}$. In this paper, the m evaluation schemes represent the number of sea surface targets, and n=7 in the evaluation indicator set, represents the 7 evaluation indicators considered in this paper, namely, target category, target distance, target heading, target speed, collision risk, AIS response status, and target typical intention. Since this paper has established a threat affiliation function for each evaluation indicator, the value of the evaluation indicator x_{ij}^t has been standardized to between 0 and 1.

According to the definition of information entropy, the information entropy of each indicator at time t is calculated:

$$E_j^t=-(\ln m)^{-1}\sum_{i=1}^{m}p_{ij}^t\ln p_{ij}^t \tag{13}$$

Where, $p_{ij}^t=\dfrac{x_{ij}^t}{\sum_{i=1}^{m}x_{ij}^t}$, if $p_{ij}^t=0$, then $p_{ij}^t\ln p_{ij}^t=0$.

Based on the information entropy of each indicator at time t, the weight of each indicator at time is calculated:

$$w_j^t=\frac{1-E_j^t}{m-\sum E_j^t} \tag{14}$$

Based on the threat assessment index system established in this paper and the weights of different evaluation indicators at each moment, the evaluation matrices of multiple targets are calculated to be close to the positive and negative ideal solutions respectively, and finally the target threats are comprehensively evaluated and ranked according to the relative closeness. The specific steps are as follows:

Step 1: Get the evaluation index matrix $X_t=\left(x_{ij}^t\right)_{m\times n}$ of all targets at time t, where the i row represents the evaluation scheme of target i, including the 7 evaluation index values of target i.

Step 2: Determine the positive ideal scheme x_j^{t+} and negative ideal scheme x_j^{t-} at different moments respectively. This paper stipulates that the positive ideal scheme is [1, 1, 1, 1, 1, 1, 1] and the negative ideal scheme is [0, 0, 0, 0, 0, 0, 0], because the 7 evaluation indicators of this paper have been standardized to [0, 1] through the threat affiliation function, and the larger the value, the higher the threat level.

Step 3: Calculate the gray correlation between different evaluation schemes and positive and negative ideal schemes. Calculate the gray correlation coefficient between the i evaluation scheme at time t and the positive and negative ideal schemes about the index j, as shown below.

$$\gamma_{ij}^{t+}=\frac{\min_i\min_j\left|x_{ij}^t-x_j^{t+}\right|+\rho\max_i\max_j\left|x_j^{t+}-x_{ij}^t\right|}{\left|x_j^{t+}-x_{ij}^t\right|+\rho\max_i\max_j\left|x_j^{t+}-x_{ij}^t\right|} \tag{15}$$

$$\gamma_{ij}^{t-}=\frac{\min_i\min_j\left|x_{ij}^t-x_j^{t-}\right|+\rho\max_i\max_j\left|x_j^{t-}-x_{ij}^t\right|}{\left|x_j^{t-}-x_{ij}^t\right|+\rho\max_i\max_j\left|x_j^{t-}-x_{ij}^t\right|} \tag{16}$$

Among them, ρ is the discrimination coefficient, $\rho\subset[0, 1]$. Based on the grey correlation coefficient, combined with the calculated index weights, the grey correlation degree r_i^{t+} and r_i^{t-} of the i-th evaluation scheme at the time t about the j-th index is further calculated.

$$r_i^{t+}=\sum_{j=1}^{n}\omega_j^t\gamma_{ij}^{t+}\quad i=1,2,\cdots,m \tag{17}$$

$$r_i^{t-}=\sum_{j=1}^{n}\omega_j^t\gamma_{ij}^{t-}\quad i=1,2,\cdots,m \tag{18}$$

Step 4: Based on the Euclidean distance, calculate the distances d_i^{t+} and d_i^{t-} between the i-th evaluation scheme and the positive and negative ideal schemes at time t.

$$d_i^{t+}=\sqrt{\sum_{j=1}^{n}\omega_j^t\left(x_{ij}^t-x_j^{t+}\right)^2} \tag{19}$$

$$d_i^{t-}=\sqrt{\sum_{j=1}^{n}\omega_j^t\left(x_{ij}^t-x_j^{t-}\right)^2} \tag{20}$$

Step 5: Calculate the closeness between the evaluation scheme and the positive and negative ideal solutions, and perform dimensionless processing on the grey correlation degree and distance.

$$\begin{aligned}&D_i^{t+}=\frac{d_i^{t+}}{\max_i\left(d_i^{t+}\right)},D_i^{t-}=\frac{d_i^{t-}}{\max_i\left(d_i^{t-}\right)},\\&R_i^{t+}=\frac{r_i^{t+}}{\max_i\left(r_i^{t+}\right)},R_i^{t-}=\frac{r_i^{t-}}{\max_i\left(r_i^{t-}\right)}\end{aligned} \tag{21}$$

Step 6: Perform weighted summation of dimensionless Euclidean distance and grey correlation. When the values of D_i^{t-} and R_i^{t+} are larger, the evaluation scheme is closer to the positive ideal solution, indicating that the threat level of target i is greater; on the contrary, when the values of D_i^{t+} and R_i^{t-} are larger, the evaluation scheme is closer to the negative ideal solution, indicating that the threat level of target is smaller. Further, the Euclidean distance and grey correlation are fused in the following way.

$$E_i^{t+} = \beta_1 D_i^{t-} + \beta_2 R_i^{t+}, \quad E_i^{t-} = \beta_1 D_i^{t+} + \beta_2 R_i^{t-} \quad (22)$$

Where, β_1 and β_2 are the preference coefficient, $\beta_1+\beta_2=1, \beta_1, \beta_2 \in [0, 1]$

Step 7: Obtain the relative closeness of the comprehensive Euclidean distance and grey correlation degree by weighted method. The relative closeness of the i-th evaluation scheme at time t is:

$$Z_i^t = \frac{E_i^{t+}}{E_i^{t+} + E_i^{t-}} \quad i = 1, 2, \cdots, m \quad (23)$$

Then, the relative proximity of different targets at time is obtained, and the threats of different targets are further ranked according to the size of the relative proximity.

4 Data Generation

This paper develops an unmanned boat confrontation simulation system based on Unity 3D, which includes 3D models of 1 unmanned boat, 25 typical sea surface ship targets, 2 islands, 1 buoy, etc. It can display the motion status of multiple unmanned boats and typical ship targets in real time, display and access the visible light and infrared pod image data of the unmanned boat, and simulate the echo data of the unmanned boat's navigation radar.

Fig.13 shows the unmanned boat confrontation simulation system. The main interface includes the message command display area, parameter setting area, global situation display area, and unmanned boat visual display area (including visible light, infrared, and radar simulation data). In the simulation system, different sea conditions can be set, as well as complex weather scene simulations such as rain and fog, to be closer to the real sea environment. The control parameters of the unmanned boat and the sea surface target can be pre-set by the program control, real-time manual control using the handle, or real-time protocol control through the TCP protocol. The simulation system can output the motion status of all unmanned boats and sea surface targets, including position coordinates, speed, direction and other information, and save them as json format files; at the same time, the visible light, infrared and radar simulation data from the perspective of the unmanned boat can also be output in the form of video streams through the RTSP protocol, or can be directly saved on the server hard disk. The confrontation simulation system supports the third-party 3D free perspective to view the real-time scene operation status, as well as the global situation perspective from a bird's-eye view. The confrontation simulation system supports reading json data files to review and demonstrate the scene, which is convenient for experimental verification.

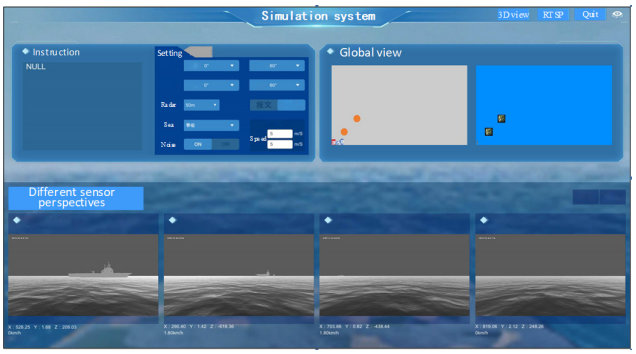

Fig.13 Simulation system interface

The intention recognition data set in this paper is generated in the unmanned boat confrontation simulation system. The real intention of the operator responsible for controlling the sea surface target is used as the true value of the intention data. The system sets the red and blue sides to generate data. The schematic diagram of the intention recognition data generation process is shown in Fig.14. First, define the rule form of assault, interception, harassment, tracking, retreat and other intentions; secondly, the movement of the sea surface target (blue side) is controlled by a group of personnel using handles respectively, and the movement of the unmanned boat escort formation (red side) is pre-set by the program or manually controlled by another group of personnel. The relative position of our unmanned boat and the target can be seen from a global perspective; the unmanned confrontation simulation system will automatically record the movement status of our unmanned boat and other sea surface targets, including coordinate position, movement speed and movement direction; after completing the generation of a set of data, save the set of data in json data format. A total of 4000 data were recorded. In the training set, the numbers of assault, interception, harassment, tracking, retreat, and other intentions were 520, 468, 461, 468, 424, and 459 respectively, and the total number of data in the training set was 2800; in the test set, the numbers of assault, interception, harassment, tracking, retreat, and other intentions were 194, 196, 201, 218, 197, and 190 respectively, and the total number of data in the test set was 1196.

Threat assessment algorithm verification data is also generated in the unmanned boat confrontation simulation system. The movement status of our unmanned boat formation and sea surface targets are recorded in the json file. It is worth noting that our formation has a total of 5 targets, consisting of 1 escort target and 4 escort boats (USV1, USV2, USV3, USV4). The operator responsible for controlling the sea surface target will record the operator's true intentions and corresponding times at different times, such as raids, retreats, and passing voyages without tactical intentions.

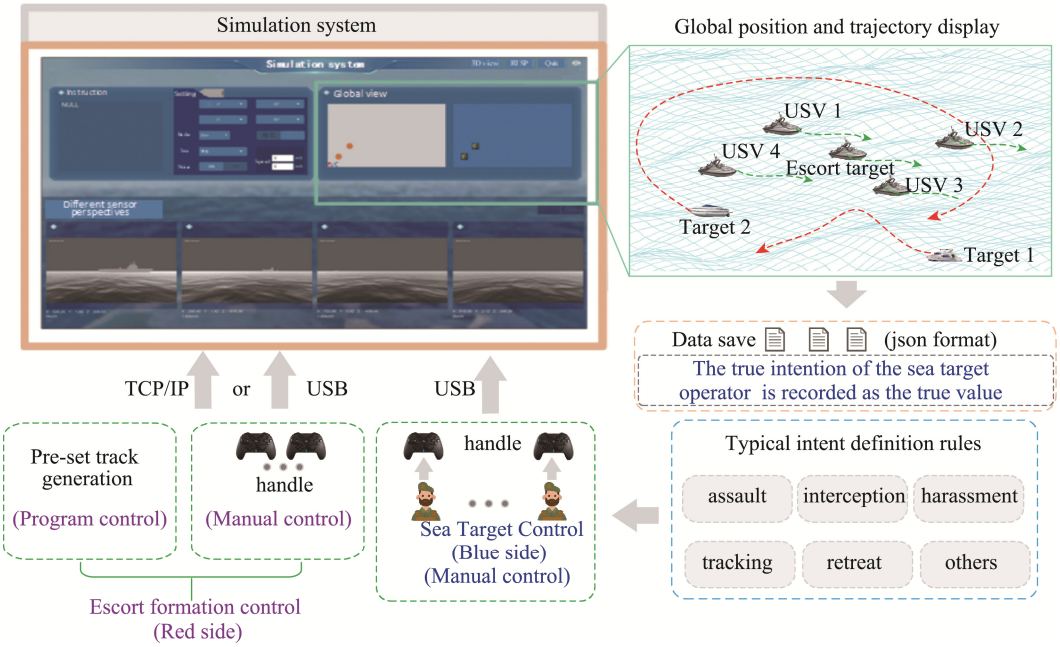

Fig.14 Schematic diagram of intent recognition data generation process

5 Results

This section verifies the threat assessment algorithm. First, we analyze the impact of different factors on the threat assessment results. Second, we verify the scientificity and rationality of the threat assessment algorithm in a typical multi-target scenario. The relative closeness calculated in this paper is the relative value of the threat. This paper focuses more on the threat ranking of different targets, timely identifying and responding to fast and hidden raid target threats, and more accurately determining which targets or areas require more attention and resources, providing important decision-making basis and helping to formulate effective defense strategies or countermeasures.

5.1 Analysis of the impact of different factors on threat assessment

5.1.1 Impact of intent recognition results

Fig.15(a) shows the motion trajectory of the unmanned boat formation and two sea targets within 40 seconds. Target 1 has the characteristics of repeated approach and distance, and target 2 first moves slowly and then moves away from the unmanned boat formation. Targets 1 and 2 are both speedboats. At the end of the track of the two targets, the positive direction of the axis is taken as 0°, and the counterclockwise directions are 0-360°. The position, speed, and direction of target 1 are (1918 m, 1566 m), 30 m/s, and 33°, respectively, and the position, speed, and direction of target 2 are (1918 m, 434 m), 30 m/s, and 327°, respectively. It can be found that targets 1 and 2 have mirrored motion states relative to the unmanned boat formation, and AIS can identify them. Without considering the intention factor, according to the threat affiliation function characteristics of the other six factors, the relative closeness of target 1 and target 2 at the end of the track should be the same, that is, the evaluation result shows that the two targets have the same threat level. However, due to the repeated changes in distance, heading, and relative speed of target 1 relative to the unmanned boat formation, the movement of target 1 has greater uncertainty, while the movement of target 2 is relatively stable. Therefore, target 1 should pose a greater threat to the escort target than target 2.

The algorithm model in this paper can judge the target threat more objectively by considering the historical state of the target, defining and identifying the typical intention of the target. As shown in Fig.15(b), the intention recognition model in this paper identifies the intention of target 1 as harassment at the 15th second, with a threat affiliation of 0.6; at the 15th second, it identifies the intention of target 2 as tracking, with a threat affiliation of 0.4, and at the 35th second, it identifies the intention of target 2 as retreat, with a threat affiliation of 0.2. Fig.15(c) and (d) are the relative proximity estimation results of different targets and the threat ranking results of different targets of the algorithm in this paper, respectively. The larger the value of the target threat ranking result, the higher the threat level. For example, the threat degree of the target ranked 2 is higher than that of the target ranked 1. From the 1st to the 7th second, the algorithm determines that the relative proximity of target 2 is higher than that of target 1. This is because target 1 is far away from the unmanned boat formation during this period, and the relative heading angle is also larger, which is in line with the objective situation. After the 7th second, as target 1 began to move toward the unmanned boat formation, the distance, heading, and relative speed of target 1 relative to the unmanned boat formation began to change repeatedly, and the relative closeness of target 1 was always higher than that of target 2. At the 40th second, at the end of the track, the relative closeness of target 1 was about 0.12 higher than that of target 2. Based on the above analysis, it

is shown that the intention recognition model in this paper can give accurate intention judgments based on the historical motion state of the target, and can more scientifically and reasonably calculate the relativecloseness of different targets and sort the target threats. The threat assessment results are consistent with the objective situation.

5.1.2 Effect of distance

This paper analyzes the influence of distance factors on threat assessment results, and the results are shown in Fig.16. Fig.16(a) shows the motion trajectory of the unmanned boat formation and two sea targets within 20 seconds. Target 1 and target 2 are heading towards the unmanned boat formation from different directions and positions at the same speed. Targets 1 and 2 are both speedboats. The positive direction of the axis is 0°, and the counterclockwise direction is 0-360°. The initial position, speed, and direction of target 1 are (2200 m, 1500 m), 20 m/s, and 225°, respectively. The position, speed, and direction of target 2 are (2500 m, 200 m), 20 m/s, and 135°, respectively. Both targets AIS respond. Fig.16 (b) and (c) are the relative closeness estimation results and threat ranking results of different targets of the proposed algorithm, respectively. As time goes by, the relative closeness of the two targets tends to increase, and the relative closeness of target 1 is always higher than that of target 2. Therefore, the threat level of target 1 is always higher than that of target 2, and the ranking results are consistent with the objective situation.

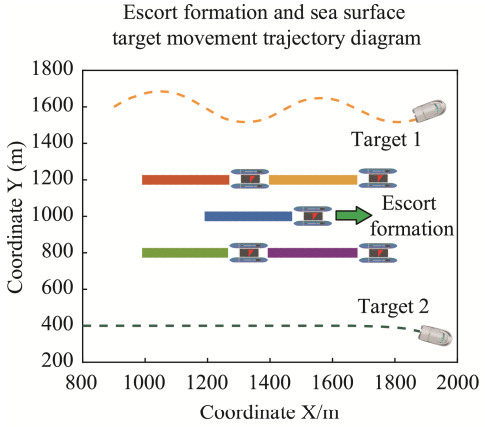

(a) The trajectory

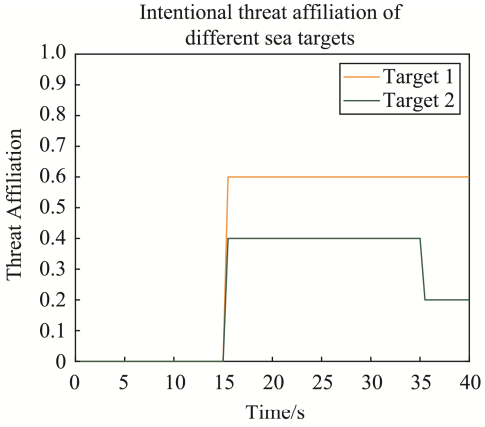

(b) Threat affiliation

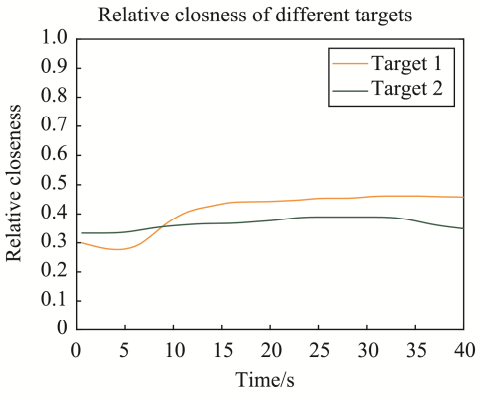

(c) Relative closeness

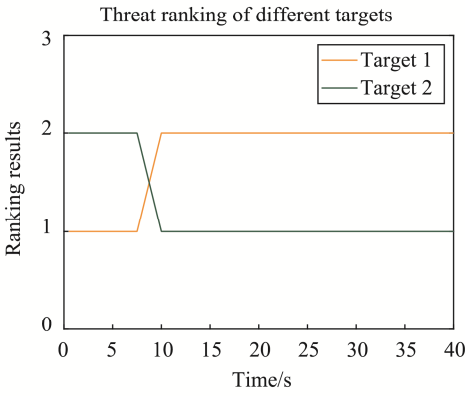

(d) Threat ranking results

Fig.15 Analysis of the impact of intent recognition results on threat assessment results

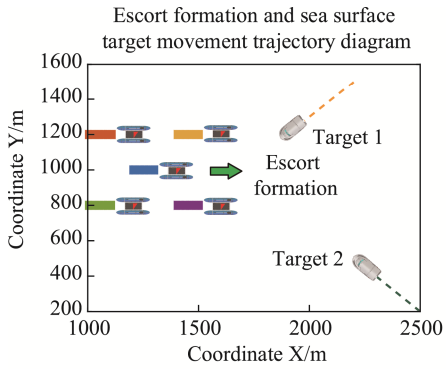

(a) The trajectory

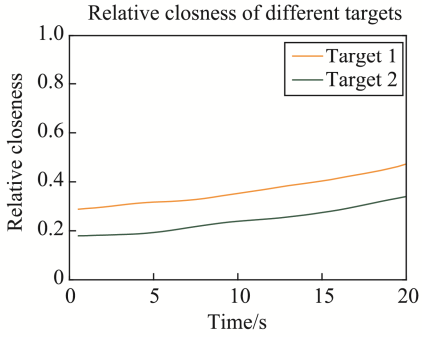

(b) Relative closeness

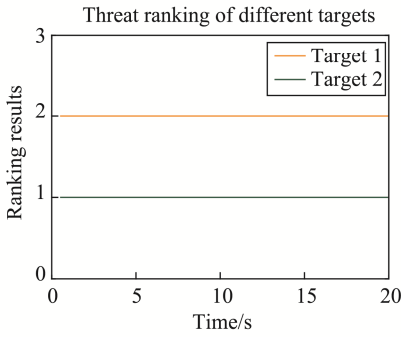

(c) Threat ranking results

Fig.16 The impact of distance on threat assessment results

5.1.3 Influence of heading

This paper analyzes the impact of target heading on threat assessment results, and the results are shown in Fig.17. Fig.17(a) shows the motion trajectory of the unmanned boat formation and two sea targets within 20 seconds. From the 1st to the 10th second, target 1 and target 2 respectively sailed towards the unmanned boat formation from different positions and at the same speed. Targets 1 and 2 are both speedboats. The positive direction of the axis is 0°, and the counterclockwise direction is 0-360°. The initial position, speed, and direction of target 1 are (2500 m, 1800 m), 20 m/s, and 225°, respectively. The position, speed, and direction of target 2 are (2500 m, 200 m), 20 m/s, and 135°, respectively. Both targets AIS responded. The heading and speed of target 1 remain consistent. At the 10th second, target 2 adjusts its direction to 180° and maintains this direction until the end of the 20-second track.

Fig.17 (b) and (c) are the relative closeness estimation results and threat ranking results of different targets of the proposed algorithm, respectively. Since target 1 and target 2 have mirrored motion states relative to the unmanned boat formation during the period of 1-10 seconds, the heading angle threat affiliation is the same, and since the AIS and intention elements are the same, the two targets have the same relative closeness. After the 10th second, due to the turn of target 2, the relative heading angle between target 2 and the unmanned boat formation is 180°, so the heading angle threat affiliation becomes 0. After target 2 turns, the threat degree of target 2 is lower than that of target 1, which is consistent with the objective situation.

5.1.4 Speed Impact

This paper analyzes the impact of target speed on threat assessment, and the results are shown in Fig.18. Fig.18 (a) shows the motion trajectory of the unmanned boat formation and two sea targets within 20 seconds. Targets 1 and 2 sail on both sides of the unmanned boat formation from different positions and at different speeds. Targets 1 and 2 are both speedboats. The positive direction of the axis is 0°, and the counterclockwise direction is 0-360°. The initial position, speed, and direction of target 1 are (1000 m, 1600 m), 20 m/s, and 350°, respectively. The position, speed, and direction of target 2 are (1000 m, 400 m), 20 m/s, and 10°, respectively. Both targets respond to AIS. The heading and speed of targets 1 and 2 remain unchanged for 20 seconds. Fig.18(b) and (c) show the relative closeness estimation results and threat ranking results of different targets of the proposed algorithm, respectively. At the initial moment, the positions and headings of targets 1 and 2 relative to the unmanned boat formation are mirror images, and only the speeds are different. The speed threat affiliation of target 1 is higher. The relative closeness of target 1 is higher than that of target 2 during the entire movement, which is consistent with the objective situation.

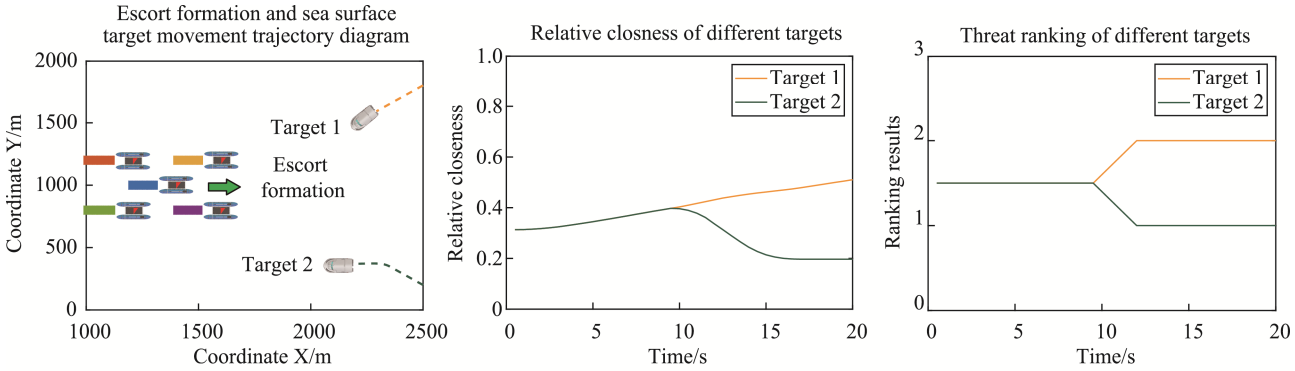

Fig.17 The impact of target heading on threat assessment results

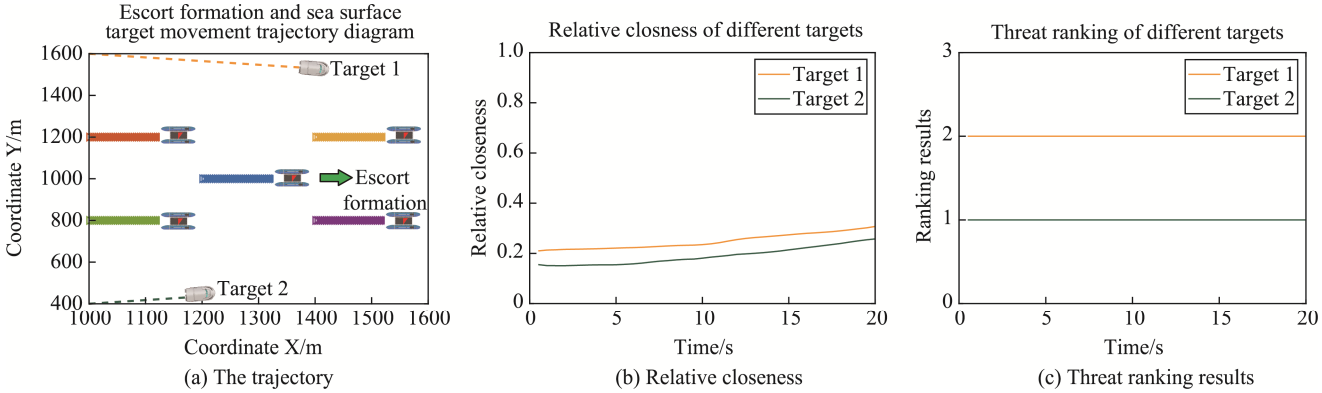

Fig.18 The impact of target speed on threat assessment results.

5.1.5 Impact of collision risk

This paper analyzes the impact of collision risk factors on threat assessment results, and the results are shown in Fig.19. Fig.19 (a) shows the motion trajectory of the unmanned boat formation and two sea targets within 20 seconds. Targets 1 and 2 sail on both sides of the unmanned boat formation from different positions and at different speeds. Targets 1 and 2 are both speedboats. The positive direction of the axis is 0°, and the counterclockwise direction is 0-360°. The initial position, speed, and direction of target 1 are (1625 m, 1800 m), 20 m/s, and 270°, respectively. The position, speed, and direction of target 2 are (1700 m, 400 m), 40 m/s, and 90°, respectively. Both targets AIS respond. The heading and speed of targets 1 and 2 are always the same as the initial state within 20 seconds. In this scenario, the target distance factor also affects the threat assessment results. By comparing the weights of different factors, it is found that the weight of the collision risk factor is higher than the distance factor weight, and it dominates in this scenario.

Fig.19(b) and (c) are the relative proximity estimation results and threat ranking results of different targets of the proposed algorithm, respectively. If target 1 does not change its motion state, target 1 will collide with the unmanned boat formation, and target 2 will not collide with the unmanned boat formation if it maintains its current motion state. Therefore, the threat level of target 1 is higher than that of target 2 during the entire motion period, which is consistent with the objective situation.

5.1.6 Impact of AIS and target type

This paper analyzes the impact of AIS response and target type on threat assessment, and the results are shown in Fig.20. Fig.20 (a) shows the motion trajectory of the unmanned boat formation and three sea surface targets within 20 seconds. Targets 1, 2, and 3 sail on both sides of the unmanned boat formation from different positions, at the same speed and in the same direction. Targets 1 and 3 are speedboats, and target 2 is a fishing boat. The positive direction of the axis is 0°, and the counterclockwise direction is 0-360°. The initial position, speed, and direction of target 1 are (1400 m, 1600 m), 7.5 m/s, and 0°, respectively, and AIS responds; the position, speed, and direction of target 2 are (1400 m, 400 m), 7.5 m/s, and 0°, respectively, and AIS responds; the position, speed, and direction of target 3 are (1000 m, 400 m), 7.5 m/s, and 0°, respectively, and AIS does not respond. The positions, speeds, and headings of targets 1 and 2 are mirror images relative to the unmanned boat formation, with only the categories being different; the positions, speeds, and headings of targets 1 and 3 are mirror images relative to the unmanned boat formation, with only the AIS responses being different. The headings and speeds of targets 1, 2, and 3 remain the same as the initial states for 20 seconds. Fig.20(b) and (c) are the relative proximity estimation results of the proposed algorithm for different targets and the threat ranking results of different targets. The threat ranking of targets 1, 2, and 3 is that target 3 has the highest threat, followed by target 1, and target 2 has the lowest threat, which is consistent with the objective situation.

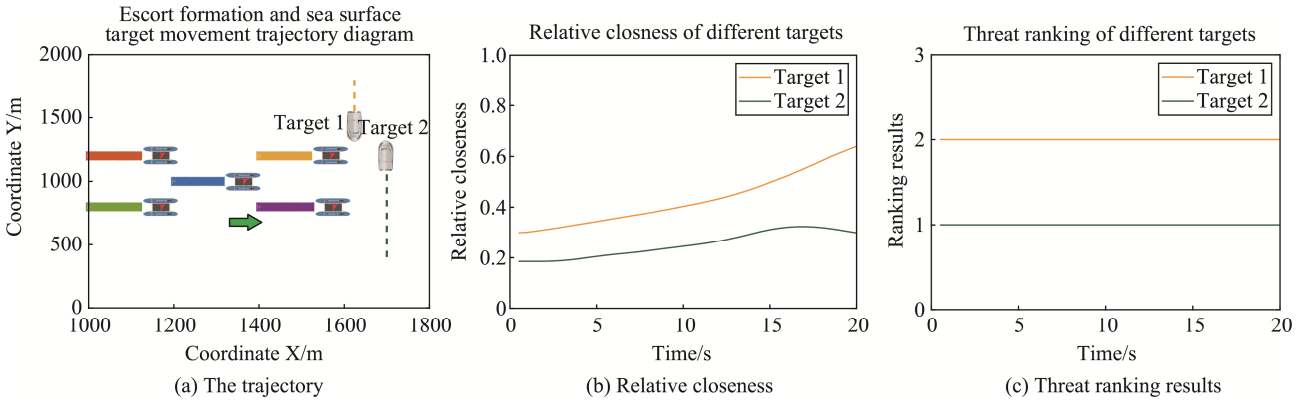

(a) The trajectory (b) Relative closeness (c) Threat ranking results

Fig.19 Impact of collision risk on threat assessment results.

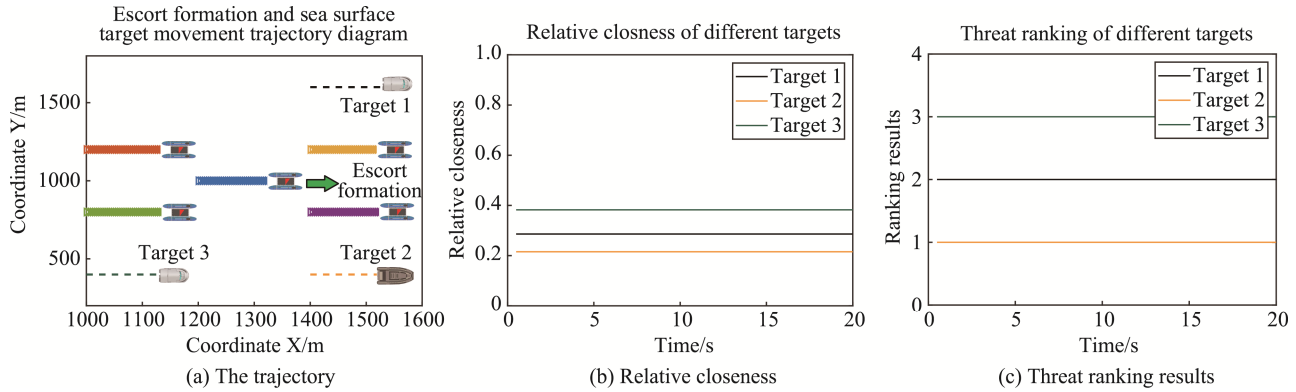

(a) The trajectory (b) Relative closeness (c) Threat ranking results

Fig.20 The impact of target type and AIS response on threat assessment results

5.2 Analysis of threat assessment results under multiple targets

Section 5.1 of this paper mainly analyzes the impact of a single major influencing factor on the target threat assessment results by setting 2 or 3 targets in each scenario. The following will design a more complex scenario to verify the scientificity and rationality of the threat assessment of the algorithm in this paper under the condition of multiple targets.

This paper uses the unmanned boat confrontation simulation system developed based on Unity3D to generate typical sea surface target scene data. There are 6 targets in the scene, and the unmanned boat formation consists of 5 unmanned boats, among which the most central one is the escort target, and the total duration is 100s. In general, target 1 is a speedboat, which was located in front of the left of the unmanned boat formation and moved in a direction of 180° in the first 20 seconds, and then turned towards the unmanned boat formation. The AIS never responded; target 2 is a speedboat, which was located in front of the right of the unmanned boat formation and moved in a direction of 180° in the first 35 seconds, and then turned towards the unmanned boat formation. The AIS never responded; target 3 is a speedboat, which was located behind the right of the unmanned boat formation and moved in a direction of 0° in the first 65 seconds, and then turned towards the unmanned boat formation. The AIS never responded; target 4 is a fishing boat, which is located behind the unmanned boat formation and moved in a direction of about 220°. The AIS can respond; target 5 is a speedboat, which is located behind the left of the unmanned boat formation and repeatedly approaches and moves away from the unmanned boat formation along the direction of 0°. The AIS never responded; target 6 is a speedboat, which is located behind the unmanned boat formation and moves in a curve at about 270°. The AIS can respond. Fig.21 shows the movement trajectory of the escort formation and the target, as well as the target's (target operator in the simulation system) true intention.

5.2.1 Threat assessment results of the algorithm in this paper

Fig.22 shows the threat assessment results of multiple targets calculated by the algorithm in this paper. Fig.22(a)-(g) show the curves of the threat affiliation functions of target distance, type, heading, speed, AIS response, intention and collision risk over time, and Fig.22(h) shows the curves of the relative proximity estimation results of different targets over time. It is worth noting that due to the Matlab drawing mechanism, when the values of multiple lines are the same, only one color can be displayed in the Matlab figure. Fig.22(b)(e) is specially explained in text. Target 4 is a fishing boat, and the rest of the targets are speedboats; Target 4 and Target 6 responded to AIS in the 5th second, and the rest of the targets did not respond, which is consistent with the situation set in the countermeasure system simulation.

In terms of target intention recognition, it can be seen from Fig.22(f) that the intention recognition method of this paper can effectively perform typical intention recognition based on the movement of the target and the unmanned boat formation. For example, targets 1 and 2 are judged as assault intentions at 35 seconds and 43 seconds respectively, and are given a higher threat affiliation. Target 3 is judged as tracking at 15 seconds and assault intention at 73 seconds. Target 5 is first judged as tracking intention and then as harassment intention, which is consistent with the real tactical intention of the target (target operator in the deduction system). When targets 1, 2, and 3 are launching a surprise attack, the algorithm of this paper can promptly find the surprise target among all targets, and make a reasonable target threat ranking based on the target speed, distance, etc., highlighting the most dangerous and important targets. According to Fig.22(i), within 0-30 seconds, since target 5 is close to the unmanned boat formation and its intention is judged to be tracking and then harassing, it has the highest threat level; when target 1 launches a surprise attack, the algorithm determines that target 1 has the highest threat level at 38-43 seconds; then, since target 2 launches a surprise attack and target 2 has a higher speed than target 1, the algorithm determines that target 2 has the highest threat level; after target 2 retreats, target 3 launches a surprise attack and target 3 has a higher speed than target 1, so target 3 has the highest threat level. The threat assessment results of the algorithm are consistent with the objective situation, which proves the scientificity and rationality of the algorithm in this paper.

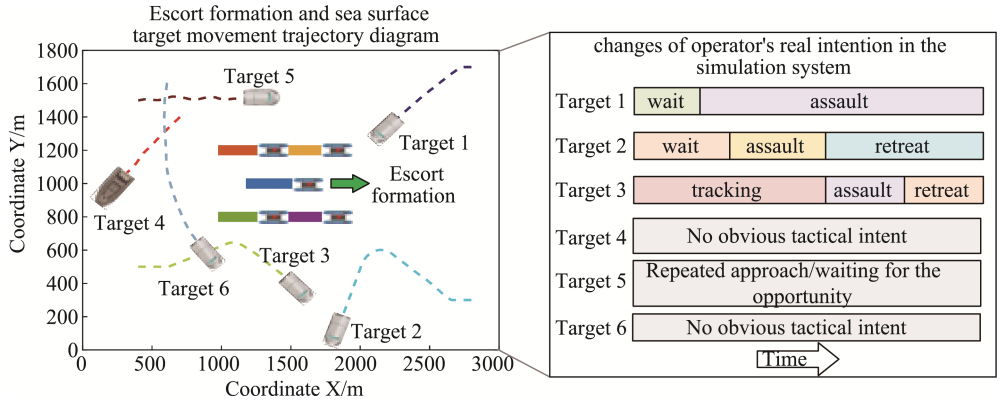

Fig.21 Escort formation and target trajectory diagram and the target's (target operator in the simulation system) real intention

5.2.2 Comparative analysis of threat assessment results with other methods

To further verify the effectiveness of the proposed algorithm, the CRITIC-TOPSIS method[49] was selected as the comparison algorithm.

Fig.23 shows the target threat assessment result of the CRITIC-TOPSIS method for the scene in Fig.21. It can be seen that when target 1 launches a surprise attack, the CRITIC-TOPSIS method can give target 1 a higher relative closeness. However, when target 3 launches a surprise attack at 65 seconds and its speed is higher than that of target 1, the algorithm fails to improve the relative closeness of target 3 and ranks its threat level third. The algorithm fails to make a reasonable judgment.

In order to further intuitively compare the threat assessment results of the algorithm in this paper and the comparison algorithm, the target state and the relative closeness estimation results of the algorithm at the 49th and 76th seconds of the scene in Fig.21 are compared respectively. Fig.24 shows the target motion trajectory at t=49 s and t=76 s.

Table 2 shows the target state at t=49 s and the relative closeness estimation results of different methods. At t=49 s, targets 1 and 2 in the unmanned boat confrontation simulation system launched a surprise attack on the unmanned boat escort formation. Target 2 is closer to the unmanned boat formation than target 1, and the speed of target 2 is 37 m/s, which is higher than 8 m/s of target 1. Target 2 should have a higher threat than target 1.

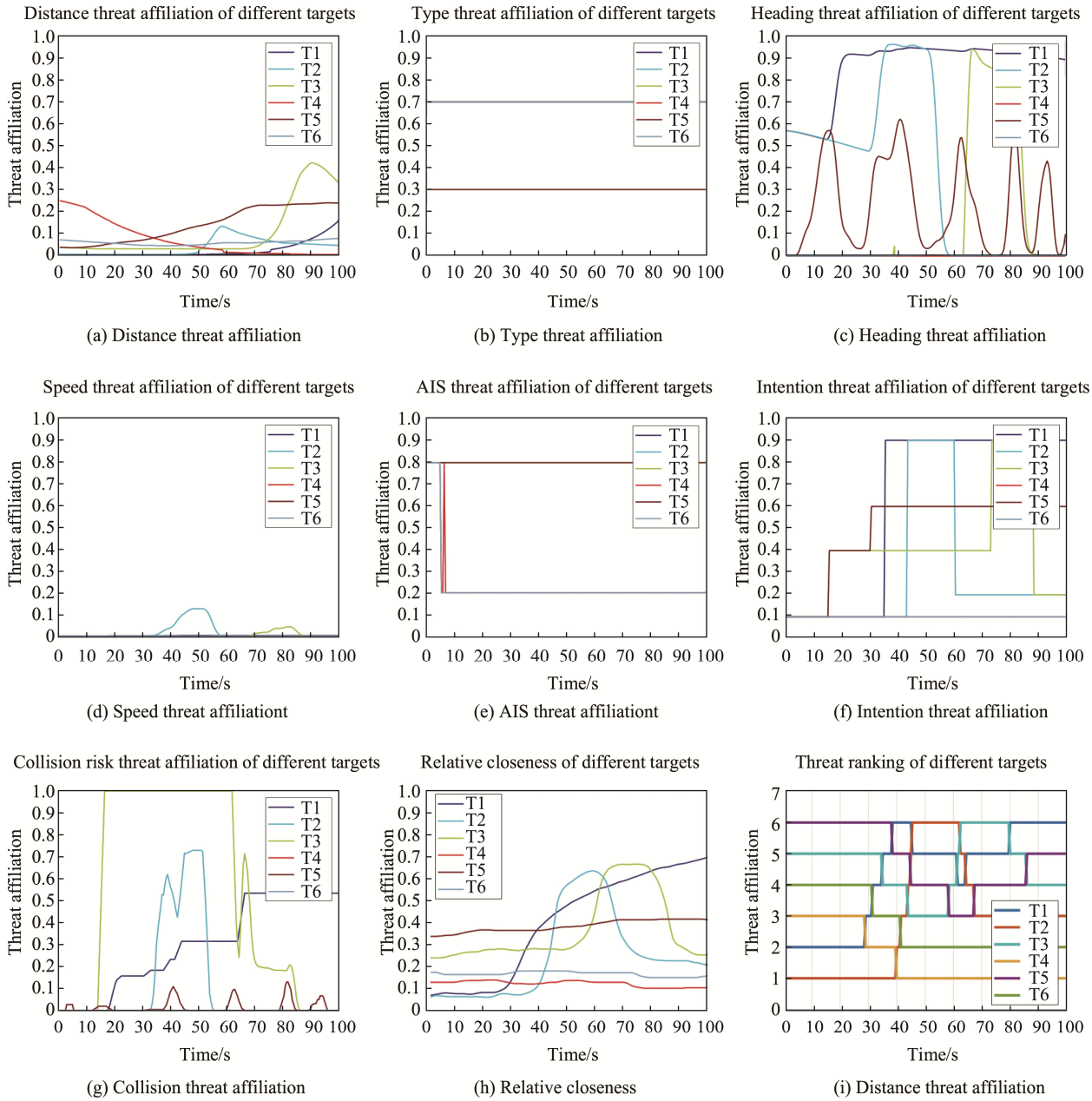

(a) Distance threat affiliation (b) Type threat affiliation (c) Heading threat affiliation

(d) Speed threat affiliationt (e) AIS threat affiliationt (f) Intention threat affiliation

(g) Collision threat affiliation (h) Relative closeness (i) Distance threat affiliation

Fig.22 Multiple target threat assessment results

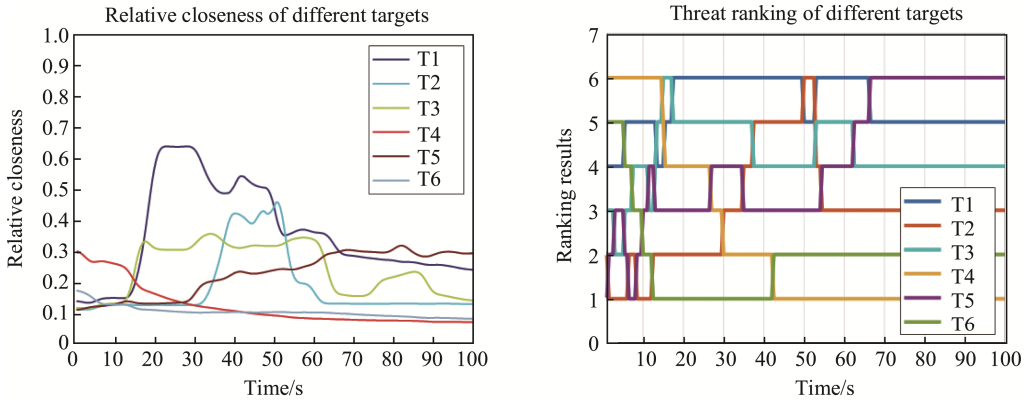

(a) Relative closeness (b) Threat ranking results

Fig.23 Threat assessment results of the comparison algorithm

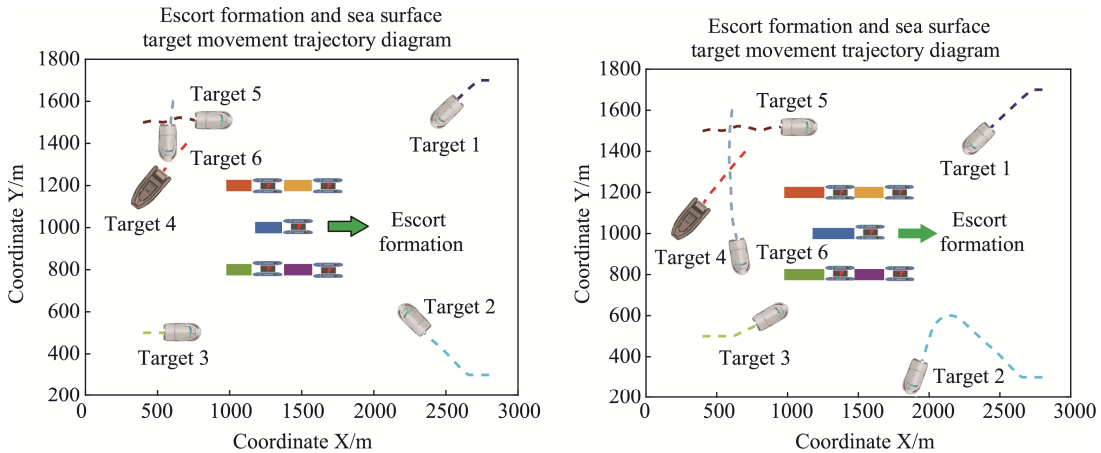

(a) t=49 seconds (b) t=76 seconds

Fig.24 Target motion trajectory at two different times

Table 2 Target status and threat assessment results of different methods (t=49 s)

ID	Type	Coordinate (m)	Heading (degree)	Speed (m/s)	Collision risk	Intention	AIS	Relative closeness of different methods	
								Proposed method	CRITIC-TOPSIS
1	Speedboat	(2550,1592)	216.0	8.0	0.1705	assault	No	0.4713	0.5084
2	Speedboat	(2292,528)	147.0	37.0	0.0068	assault	No	0.5650	0.4053
3	Speedboat	(556,500)	0.0	4.0	0.0047	tracking	No	0.2737	0.3224
4	Fishing boat	(494,1226)	219.0	6.0	0.0089	others	Yes	0.1321	0.0994
5	Speedboat	(844,1510)	12.0	10.0	0.0385	harassment	No	0.3772	0.2420
6	Speedboat	(586,1390)	270.0	12.0	0.0110	others	Yes	0.1757	0.1091

According to the typical target intention recognition model of this paper, targets 1 and 2 are correctly identified as assault intentions, target 5 is correctly identified as harassment intentions, and target 3 is correctly identified as tracking intentions. The speeds of target 5 and target 3 are 10 m/s and 4 m/s respectively. Considering the uncertainty of the motion trajectory of target 5 (repeatedly approaching and moving away from the unmanned boat formation), target 5 should have a higher threat than target 3. Let m_i represent the relative closeness value of the i-th target. According to the algorithm of this paper, the relative closeness is calculated. According to the size of the relative closeness, the threat ranking result of the target by the algorithm of this paper can be obtained as follows: $m_2>m_1>m_5>m_3>m_6>m_4$, while the relative closeness of the target is calculated according to the CRITIC-TOPSIS method, and the threat ranking result of the target is obtained according to the size of the relative closeness: $m_1>m_2>m_3>m_5>m_6>m_4$. By considering 7 evaluation indicators and assigning reasonable weights,

the algorithm of this paper correctly makes the following judgments: the threat of target 2 is higher than that of target 1, the threat of target 5 is higher than that of target 3, and target 2 is in a state of surprise attack and has the highest threat, which is consistent with the above analysis and the objective situation of this scene in the unmanned boat confrontation simulation system. The CRITIC-TOPSIS algorithm determines that the threat of target 2 is lower than that of target 1, and the threat of target 5 is lower than that of target 3. Due to the confusion of the weighting of the evaluation indicators, the CRITIC-TOPSIS algorithm fails to make a reasonable target threat estimate. In summary, the algorithm in this paper can more scientifically calculate the relative proximity of the target and automatically make a more reasonable target threat ranking judgment, and timely warn the raid targets with higher threat.

Table 3 shows the target state at t=76 s and the relative closeness estimation results of different methods. At t=76 s, targets 1 and 3 in the unmanned boat confrontation simulation system launched a surprise attack on the unmanned boat escort formation. Target 3 is closer to the unmanned boat formation than target 1, and the speed of target 3 is 31 m/s, which is higher than the 8 m/s of target 1. Target 3 should have a higher threat than target 1; the motion trajectory of target 5 is uncertain (repeatedly approaching and moving away from the unmanned boat formation). Compared with target 2, it is closer to the unmanned boat formation, and target 2 is in retreat and gradually moving away from the unmanned boat formation. Therefore, target 5 should have a higher threat than target 2. According to the typical target intention recognition model in this paper, targets 1 and 3 are correctly identified as assault intentions, target 5 is correctly identified as harassment intentions, and target 2 is correctly identified as retreat intentions. According to the size of the relative closeness, the result of the target threat ranking of the algorithm in this paper is: $m_3>m_1>m_5>m_2>m_6>m_4$, and according to the CRITIC-TOPSIS method, the relative closeness of the target is calculated, and the result of the target threat ranking according to the size of the relative closeness is: $m_3>m_1>m_5>m_2>m_6>m_4$. By considering 7 evaluation indicators and assigning reasonable weights, the algorithm in this paper correctly makes the following judgments: the threat of target 3 is higher than that of target 1, the threat of target 5 is higher than that of target 2, and target 3 is in a surprise attack state and has the highest threat, which is consistent with the above analysis and the objective situation of this scene in the unmanned boat confrontation simulation system. However, the CRITIC-TOPSIS algorithm determines that the threat of target 3 is lower than that of target 5 and target 1. Due to the confusion of the weighting of the evaluation indicators, the CRITIC-TOPSIS algorithm fails to make a reasonable target threat estimate. In summary, the algorithm in this paper can calculate the relative closeness of the target more scientifically and automatically make a more reasonable target threat ranking judgment, and timely warn the surprise targets with higher threat levels.

Table 3 Target status and threat assessment results of different methods (t=76 s)

ID	Type	Coordinate (m)	Heading (degree)	Speed (m/s)	Collision risk	Intention	AIS	Relative closeness of different methods	
								Proposed method	CRITIC-TOPSIS
1	Speedboat	(2370,1470)	216.0	8.0	0.2889	assault	No	0.6140	0.2803
2	Speedboat	(1882,228)	246.0	9.0	0.0026	retreat	No	0.2431	0.1359
3	Speedboat	(842,574)	18.0	31.0	0.3230	assault	No	0.6630	0.2015
4	Fishing boat	(394,1134)	231.0	4.0	0.0059	others	Yes	0.0995	0.0825
5	Speedboat	(1080,1510)	6.0	5.0	0.0279	harassment	No	0.4098	0.3020
6	Speedboat	(658,926)	291.0	10.0	0.0068	others	Yes	0.1533	0.0985

6 Conclusion

In order to solve the problem of insufficient target information mining and failure to consider the historical motion state of the target in target threat assessment, this chapter establishes a threat assessment model that considers the instantaneous state and historical state of the target. The instantaneous state of the target considers six evaluation indicators, including target category, target distance, target heading, target speed, collision risk, and AIS response status; a target typical intention recognition model based on historical state is established, and a typical intention recognition method based on graph neural network is proposed to capture the dynamic correlation characteristics between the target and the escort formation, realize end-to-end target typical intention recognition, and use the intention recognition result as an evaluation indicator of the threat assessment model. Then, threat affiliation functions are established for the seven evaluation indicators respectively, and the evaluation indicators are weighted based on multi-attribute decision analysis, and then the relative closeness between the evaluation schemes of different

targets and the positive and negative ideal schemes is calculated, and the target threat ranking is determined based on the relative closeness. This chapter designs and develops an unmanned boat confrontation simulation system, and generates a typical intention recognition data set and threat assessment scenario simulation data through real-life confrontation. The simulation experiments verified the excellent performance of the proposed method in identifying typical target intentions. The comparative analysis showed that the proposed method can timely detect surprise target threats and give scientific and reasonable target threat ranking results. In the future, the proposed method will be implemented in the real scene with USVs in the sea to test the practicality of proposed method. Besides, more comparative methods will be implemented to make our results more credible. Furthermore, more factors will be considered in the threat assessment method, such as weapon or the size of targets, to make the evaluation results more fair and objective.

Author Contributions:

Conceptualization, Data curation, Formal analysis: Peng Wu; Funding acquisition, Investigation, Methodology: Bei Sun and Shaojing Su; Project administration, Resources, Software: Xiaoyong Sun; Supervision, Validation, Roles/ Writing-original draft; and Writing - review & editing: Zhen Zuo.

Funding Information:

This research was funded by by the National Natural Science Foundation of China under Grant 52101377.

Data Availability:

The authors declare that the main data supporting the findings of this study are available within the paper and its Supplementary Information files.

Conflict of Interest:

The authors declare no competing interests.

Dates:

Received 25 September 2024; Accepted 13 October 2024; Published online 17 October 2024.

References

[1] Wang Guangyuan, Li Haomin, Zhu Dacheng, et al. Threat assessment of sea surface targets based on entropy weight method-grey correlation method[J]. Command Control and Simulation, 2023, 45(4): 57-61.

[2] Shu Jiansheng, Lai Xiaochang, Li Yaxiong, et al. Threat level assessment model of mobile targets at sea based on APSO and FCM[J]. Firepower and Command Control, 2023, 48(8): 74-80.

[3] Li Zhe. Research on target grouping and group situation threat analysis model for sea and air targets[D]. Xidian University, 2021.

[4] Chen X, Zhang B, Liu W, et al. Threat Assessment of the Maritime Targets Based on Dynamic Bayesian Networks[C]. 2022 34th Chinese Control and Decision Conference (CCDC), Hefei, China, 2022: 4841-4846.

[5] Guo Yuanyuan. Research on dynamic fusion target threat assessment based on interval intuitionistic fuzzy multi-attribute decision making[D]. Dalian University, 2019.

[6] Chen Xingle, Huang Yanyan, Chen Tiande. Threat level assessment of offshore threat targets and allocation of unmanned boat forces[J]. Firepower and Command Control, 2022, 47(3): 73-81.

[7] Gong H, Yu X, Zhang Y, et al. Dynamic Threat Assessment of Air multi-target Based on DBN-TOPSIS Method. 2021 China Automation Congress (CAC)[C]. 2021: 6902-6907.

[8] Zhao R, Yang F, Ji L, et al. Dynamic Air Target Threat Assessment Based on Interval-Valued Intuitionistic Fuzzy Sets, Game Theory, and Evidential Reasoning Methodology [J]. Mathematical Problems in Engineering, 2021, 2021: 1-13.

[9] Shi W, Li H, He W, et al. Threat Assessment of Air Targets Based on Intent Prediction[C]. 2021 IEEE 5th Information Technology,Networking,Electronic and Automation Control Conference (ITNEC), Xi'an, China, 2021: 311-321.

[10] Chen Kaiyuan, Song Yuan. Analysis of threat assessment index system for sea surface targets[J]. Ship Electronic Engineering, 2009, 29(6): 66-70.

[11] Gao Y, Lv N. Multi-target Threat Assessment Method Based on An Effective Reduction Method. 2022 8th International Conference on Systems and Informatics (ICSAI)[C]. 2022: 1-5.

[12] Zhang H, Wei Z. Research on Armored Unit Target Threat Assessment Based on SVM. 2022 IEEE 10th Joint International Information Technology and Artificial Intelligence Conference (ITAIC)[C]. 2022: 2072-2074.

[13] Wang Changjin, Zhang Yonghui, Huang Bin. Key point air defense threat assessment based on grey fuzzy matter-element analysis[J]. Firepower and Command Control, 2013, 38(8): 47-50+54.

[14] Lin Z, Zhishu Y, Wenxin F. Research on Threat Assessment Based on Intuitionistic Fuzzy Set Theory[C]. 2009 International Conference on Intelligent Human-Machine Systems and Cybernetics, Hangzhou, Zhejiang, China, 2009: 494-499.

[15] Hong L, Bailin L, Ruiqi S. Air Attack Target Threat

Assessment Based on Combination Weighting[J]. International Journal of Advanced Network, Monitoring, and Controls, 2023, 7(2): 92-99.

[16] Yu D, Wang H, Li B, et al. PROMETHEE-Based Multi-AUV Threat Assessment Method Using Combinational Weights[J]. Journal of Marine Science and Engineering, 2023, 11(7): 1422.

[17] Basso Brancalion J F, Kienitz K H. Threat Evaluation of Aerial Targets in an Air Defense System Using Bayesian Networks[C]. 2017 IEEE 15th Intl Conf on Dependable, Autonomic and Secure Computing, 15th Intl Conf on Pervasive Intelligence and Computing, 3rd Intl Conf on Big Data Intelligence and Computing and Cyber Science and Technology Congress, Orlando, FL, 2017: 897-900.

[18] Azimirad E, Haddadnia J. A new model for threat assessment in data fusion based on fuzzy evidence Theory[J]. International Journal of Advances in Intelligent Informatics, 2016, 2(2).

[19] Niu S, Wang H, Gu Y, et al. Research on UUVs Swarm Threat Assessment and Strategy Selection. Global Oceans 2020: Singapore – U.S. Gulf Coast[C]. 2020: 1-6.

[20] Wang Baihe, Huang Jianguo, Zhang Qunfei. Research on target threat assessment model based on improved grey relational analysis[J]. Computer Engineering and Applications, 2008(4): 212-215.

[21] Chen Hua, Zhang Ke, Cao Jianshu. Target threat assessment based on PSO-BP algorithm[J]. Journal of Computer Application Research, 2012, 29(3): 900-901+932.

[22] Zhang Feng, Xu Wen, Wu Dongyan, et al. Research on target threat estimation based on BP-Adaboost in combat simulation[J]. System Simulation Technology, 2019, 15(3): 180-183.

[23] Xi Zhifei, Xu An, Kou Yingxin, et al. Air combat threat assessment based on improved GRA-TOPSIS[J]. Journal of Beijing University of Aeronautics and Astronautics, 2020, 46(2): 388-397.

[24] Li Ye. Research on battlefield target threat assessment method based on Bayesian network[D]. Xi'an University of Technology, 2022.

[25] Liu Fang, Zhang Yong, Gong Hua, et al. Fusion threat assessment of air targets based on DBN-TOPSIS method[J]. Journal of Ordnance Equipment Engineering, 2023, 44(1): 136-143.

[26] Zhang Kun, Zhang Zhenchong, Liu Zekun, et al. Dynamic threat assessment of multi-targets in mixed air combat based on FD-TODIM[J]. Systems Engineering and Electronics, 2023, 45(1): 148-154.

[27] X. B. Guo, Z. Wang, and W. D. Hu, “Information fusion with Bayesian networks for target recognition,” J. Syst. Simul., vol. 17, no. 11, pp. 2713-2716, Nov. 2005.

[28] A. W. Yang, L. Zhan-Wu, X. An, X. Zhi-Fei, and C. Yi-Zhe, “Threat level assessment of the air combat target based on weighted cloudy dynamic Bayesian networks,” Flight Dyn., vol. 38, no. 4, pp. 87-94, Apr. 2020.

[29] F. J. Zhao, Z. J. Zhou, C. H. Hu, L. Wang, and T. Liu, “Aerial target intention recognition approach based on belief-rule-base and evidential reasoning,” Electron. Opt. Control, vol. 24, no. 8, pp. 15-19, Aug. 2017.

[30] X. Yin, M. Zhang, and M. Q. Chen, “Combat intention recognition of the target in the air based on discriminant analysis,” J. Projectile, Rocket, Missiles Guid., vol. 38, no. 3, pp. 46-50, Jun. 2018.

[31] M. Ben-Bassat and A. Freedy, “Knowledge requirements and management in expert decision support systems for (military) situation assessment,”IEEE Trans. Syst., Man, Cybern., vol. SMC-12, no. 4, pp. 479-490, Jul. 1982, doi: 10.1109/TSMC.1982.4308852.

[32] W. Zhou, J. Zhang, N. Gu, and G. Yan, “Recognition of combat intention with insufficient expert knowledge,” in Proc. 3rd Int. Conf. Comput. Modeling, Simulation Appl. Math., Wuhan, China, Sep. 2018, pp. 328-333.

[33] X. Niu, H. Zhao, and Y. Zhang, “Naval vessel intention recognition based on decision tree,” Ordnance Ind. Autom., vol. 29, no. 6, pp. 473-482, May/Jun. 2010.

[34] X. Xia, “The study of target intention assessment method based on D-S evidence theory,” M.S. thesis, Dept. Inf. Syst. Eng., Nat. Univ. Defense Technol., Changsha, China, 2006.

[35] L. Ma, F. Tian, and H. Y. Shan, “Optimization method of surface ship to air combat deployment based on time window,” J. Phys. Conf. vol. 1574, Jun. 2020, Art. no. 012151.

[36] W. Wang, H. Hong, Y. Zhang, S. Li, and J. Shi, “Realization of real-time detection algorithms for key parts of unmanned aerial vehicle based on support vector machine,” in Proc. Autom. Target Recognit. Navigat., 2020, pp. 116-122.

[37] Jin Q, Gou X T, Jin W D, et al . Intention Recognition of Aerial Targets Based on Bayesian Optimization Algorithm[C]. 2nd IEEE International Conference on Intelligent Transportation Engineering, 2017: 356 − 359 .

[38] Q. K. Yao, S. J. Liu, X. Y. He, and W. Ou, “Research and prospect of battlefield target operational intention recognition,” J. Command Control, vol. 3, no. 2, pp. 127-131, Feb. 2017.

[39] B. Li, W. Pei, J. Li, X. Zhang, and Y. Liu, “ISAR target recognition system design based on artificial intelligence,” in Proc. Pattern Recognit. Comput. Vis., Feb. 2020, pp. 149-155.

[40] Y. Gong, Z. Ma, M. Wang, X. Deng, and W. Jiang, “A new multi-sensor fusion target recognition method based on complementarity analysis and neutrosophic set,” Symmetry, vol. 12, no. 9, p. 1435, Aug. 2020.

[41] A. Li, B. Zheng, and L. Li, “Intelligent transportation application and analysis for multi-sensor information fusion of Internet of Things,” IEEE Sensors J., vol. 21, no. 22, pp. 25035-25042, Nov. 2021.

[42] J. Pei, W. Huo, C. Wang, Y. Huang, Y. Zhang, J. Wu, and J. Yang, “Multi-view deep feature learning network for SAR automatic target recognition,”Remote Sens., vol. 13, no. 8, p. 1455, Apr. 2021.

[43] H. Chen, Q. L. Ren, and Y. Hua, “Fuzzy neural network based tactical intention recognition for sea targets,” Syst. Eng. Electron., vol. 38, no. 8, pp. 1847-1853, Aug. 2016.

[44] X. Kong, B. Cai, Y. Liu, H. Zhu, Y. Liu, H. Shao, C. Yang, H. Li, and T. Mo, “Optimal sensor placement methodology of hydraulic control system for fault diagnosis,” Mech. Syst. Signal Process., vol. 174, Jul. 2022, Art. no. 109069.

[45] B. Cai, C. Sheng, C. Gao, Y. Liu, M. Shi, Z. Liu, Q. Feng, and G. Liu, “Artificial intelligence enhanced reliability assessment methodology with small samples,” IEEE Trans. Neural Netw. Learn. Syst., early access, Nov. 25, 2021, doi: 10.1109/TNNLS.2021.3128514.

[46] T. Zhou, M. Chen, Y. Wang, J. He, and C. Yang, “Information entropy based intention prediction of aerial targets under uncertain and incomplete information,” Entropy, vol. 22, no. 3, p. 279, Feb. 2020.

[47] W. Wei and G. B. Gongbao, “Detection and recognition of air targets by unmanned aerial vehicle based on RBF neural network,” Ship Electron. Eng., vol. 38, no. 10, pp. 37-40, 2018, doi: 10.3969/j.issn.16729730.2018.10.009.

[48] Zheng Zhongyi. Research on ship automatic collision avoidance decision system[D]. Dalian Maritime University, 2000.

[49] Xu Yuheng, Cheng Siyi, Pang Mengyang. Dynamic radiation source threat assessment based on CRITIC-TOPSIS[J]. Journal of Beijing University of Aeronautics and Astronautics, 2020, 46(11): 2168-2175.